REPORT DOCUMENTATION PAGE

Form Approved
OMB No. 0704-0188

1. REPORT DATE *(DD-MM-YYYY)*	**2. REPORT TYPE**	**3. DATES COVERED** *(From - To)*
10-02-2009	Journal Article	

4. TITLE AND SUBTITLE

Atomic Spectral-Product Representations of Molecular Electronic Structure: Metric Matrices and the Spectral Compositions of Molecular Eigenfunctions (Preprint)

5a. CONTRACT NUMBER

5b. GRANT NUMBER

5c. PROGRAM ELEMENT NUMBER

6. AUTHOR(S)

M. Ben-Nun, P.W. Langhoff (UC San Diego); J.D. Mills, J.A. Boatz (AFRL/RZSA);
R.J. Hinde (University of Tennessee); C.L. Winstead (CIT); P.W. Langhoff (University of Nebraska)

5d. PROJECT NUMBER

5e. TASK NUMBER

5f. WORK UNIT NUMBER
50260541

7. PERFORMING ORGANIZATION NAME(S) AND ADDRESS(ES)

Air Force Research Laboratory (AFMC)
AFRL/RZSP
10 E. Saturn Blvd.
Edwards AFB CA 93524-7680

8. PERFORMING ORGANIZATION REPORT NUMBER

AFRL-RZ-ED-JA-2009-043

9. SPONSORING / MONITORING AGENCY NAME(S) AND ADDRESS(ES)

Air Force Research Laboratory (AFMC)
AFRL/RZS
5 Pollux Drive
Edwards AFB CA 93524-70448

10. SPONSOR/MONITOR'S ACRONYM(S)

11. SPONSOR/MONITOR'S NUMBER(S)
AFRL-RZ-ED-JA-2009-043

12. DISTRIBUTION / AVAILABILITY STATEMENT

Approved for public release; distribution unlimited (PA #09080).

13. SUPPLEMENTARY NOTES

For publication in the Journal of Physical Chemistry.

14. ABSTRACT

Recent progress is reported in development of *ab initio* computational methods for the electronic structures of molecules employing atomic spectral-product representations. In this approach, the physically significant many-electron eigenstates of constituent atoms provide a computational basis for descriptions of the electronic structure of matter as an alternative to more commonly employed atomic- or molecular-orbital-based representations. Particular attention is focused in the present report on properties of the metric matrix and on the spectral compositions of molecular eigenstates described in spectral-product representations. Concluding remarks describe briefly additional studies in progress and the prognosis for performing spectral-product calculations more generally and efficiently.

15. SUBJECT TERMS

16. SECURITY CLASSIFICATION OF:			**17. LIMITATION OF ABSTRACT**	**18. NUMBER OF PAGES**	**19a. NAME OF RESPONSIBLE PERSON**
					Dr. Jerry A. Boatz
a. REPORT	**b. ABSTRACT**	**c. THIS PAGE**	SAR	37	**19b. TELEPHONE NUMBER** *(include area code)*
Unclassified	**Unclassified**	**Unclassified**			N/A

Atomic Spectral-Product Representations of Molecular Electronic Structure: Metric Matrices and the Spectral Compositions of Molecular Eigenfunctions - Preprint†

M. Ben-Nun,[a] J.D. Mills,[b] R.J. Hinde,[c] C.L. Winstead,[d]

G.A. Gallup,[e] J.A. Boatz,[b] and P.W. Langhoff[a]

[a] San Diego Supercomputer Center and Department of Chemistry & Biochemistry, University of California, 9500 Gilman Drive, La Jolla, CA, 92093-0505

[b] Air Force Research Laboratory, 10 East Saturn Blvd., Edwards AFB, CA 93524-7680

[c] Department of Chemistry, University of Tennessee, Knoxville, TN 37996-1600

[d] A.A. Noyes Laboratory of Chemical Physics, California Institute of Technology, Pasadena, CA 91125

[e] Department of Physics and Astronomy, University of Nebraska, Lincoln, NE 68588-0111

(15 January 2009)

Author for correspondence:

Peter W. Langhoff
San Diego Supercomputer Center
University of California San Diego
9500 Gilman Drive, MS 0505
La Jolla, CA 92093-0505

(e-mail - langhoff@drifter.sdsc.edu; Fax - 858-534-4974; Phone 858-822-3611)

† Work supported in part by the US Air Force Research Laboratory

Abstract

Recent progress is reported in development of *ab initio* computational methods for the electronic structures of molecules employing atomic spectral-product representations. In this approach, the physically significant many-electron eigenstates of constituent atoms provide a computational basis for descriptions of the electronic structure of matter as an alternative to more commonly employed atomic- or molecular-orbital-based representations. The Hamiltonian matrix is seen to be a sum over atomic energies and a pairwise sum over Coulombic interaction terms which depend only on the separations of the individual atomic pairs. Overall electron antisymmetry can be enforced in the approach by unitary transformation when appropriate, rather than as a possibly encumbering or unnecessary global constraint. The matrix representative of the antisymmetrizer in the spectral-product basis, which is equivalent to the metric matrix of the corresponding explicitly antisymmetric basis, provides the required transformation to antisymmetric or linearly-independent states after Hamiltonian evaluation. Particular attention is focused in the present report on properties of the metric matrix and on the spectral compositions of molecular eigenstates described in spectral-product representations. Illustrative calculations are reported for simple but prototypically important diatomic (H_2, CH) and triatomic (H_3, CH_2) molecules employing recently devised algorithms and computer codes. This particular implementation of the approach combines valence-bond constructions of standard tableau functions and matrices with transformations to atomic eigenstate product representations, employing Slater-orbital-based one- and two-electron integral evaluations. The calculated metric matrices and corresponding potential energy surfaces obtained in this way elucidate a number of aspects of the spectral-product development, including the nature of closure in the spectral-product representation, the general redundancy of its explicitly antisymmetrized form, the convergence of the two apparently disparate descriptions to a common invariant subspace, and the manner in which a chemical bonding descriptor is provided by the atomic spectral compositions of molecular eigenstates obtained in the representation. Concluding remarks describe briefly additional studies in progress and the prognosis for performing spectral-product calculations more generally and efficiently.

I. Introduction

The electronic eigenstates of atoms provide a well-known formal basis for simple product representations of molecular electronic wave functions and interaction energies in long-range separation limits.[1] More generally, *ab initio* investigations of the electronic structures and associated potential energy surfaces of molecules tend to employ explicitly antisymmetric representations based on early molecular-orbital or valence-bond descriptions of the relevant electronic degrees of freedom.[2−5] In these approaches, the presence of the component atomic constituents is not made explicit, but is evident largely in the choices of atomic orbitals employed in the molecular representational basis sets. It has apparently proved difficult to base a general *ab initio* computational approach to the electronic structures of matter directly on an atomic representation,[6] in spite of the fact that atoms clearly comprise molecules and other forms of matter.

A recent series of reports emphasizes both the difficulties and potential advantages of adopting an atomic eigenstate-product representation in *ab-initio* calculations of molecular electronic structures.[7−11] This program of study, the motivations and purposes of which were described earlier,[12] is predicated largely on the demonstrable closure of the outer spectral product of complete constituent atomic eigenstates for representations of molecular electronic states in the absence of explicit (term-by-term) enforcement of aggregate electron antisymmetry. Although both conceptual and computational barriers must be overcome in such an approach, certain potential advantages follow from its adoption. These include the possibility of performing accurate atomic and atomic-interaction calculations once and for all and retaining such information for repeated molecular applications, employing entirely analytical methods in calculating the angular dependences of atomic interactions, and the opportunity to enforce molecular antisymmetry when required, rather than as a possibly encumbering overall global constraint, to mention some important examples.[7−12]

In the present contribution, additional theoretical aspects of the atomic spectral-product approach to molecular electronic structure are reported, the essential features of a computer code suite for performing such calculations are described, and selected computational applications to prototypically important diatomic (H_2, CH) and triatomic (H_3, CH_2) molecules

are presented. Calculations of metric matrices in these cases, and of corresponding potential energy curves and surfaces, in spectral-product representations illustrate the capabilities of the valence-bond- and Slater-orbital-based algorithms and codes devised. The metric matrices, which provide a connecting bridge between spectral-product representations in the absence or presence of term-by-term antisymmetry, clarify a number of aspects of the development, including the nature of closure in the spectral-product representation and the general redundancy of its explicitly antisymmetrized form. The calculations reported for H_2 and H_3 characterize the spectrum of the antisymmetrizer as that of a compact operator in the spectral-product representation, and demonstrate specific redundancies between commonly employed charge-transfer and one-electron covalent excitations, whereas the potential energy curves for ground and excited states demonstrate the advantages of the Slater-orbital-based integral evaluations employed. The spectral compositions of the atomic-product representations of molecular eigenfunctions are seen to provide highly satisfying descriptors of chemical bonding in CH and CH_2 molecules, which have played important historical roles in the development of accurate *ab initio* quantum methods for electronic structure and spectra.[13,14]

The theory is described in Section II, where the atomic spectral representations of aggregate electronic degrees of freedom are defined, the forms of metric and Hamiltonian matrices with and without explicit antisymmetrization are reported, and the unitary transformation formalism for isolation of the physical and linearly-independent Hamiltonian subspaces are given and their equivalence established. Calculations employing the recently devised algorithms and computer codes, reported in Section III, include metric matrices and energy eigenvalues for the aforementioned H_2, CH, H_3, and CH_2 molecules. Discussion and concluding remarks presented in Section IV describe additional studies in progress and strategies employed in performing atomic spectral-product calculations more generally and efficiently.

II. Theoretical Background and Developments

Selected background information is provided in this Section in summary of previously devised aspects of the spectral-product approach to molecular electronic structure,[7−12] and new theoretical developments and clarifications are reported. The atomic spectral-product representations of molecular electronic states of interest here are described in Section **A**, construction of Hamiltonian matrices in these representations are described in Section **B**, and the role of the aggregate metric matrix in isolation of physically significant Schrödinger eigenstates is described in Section **C**.

A. Atomic Spectral-Product Representations.

The adiabatic (Born-Oppenheimer) electronic states obtained from solution of the non-relativistic Schrödinger equation

$$\hat{H}(\boldsymbol{r} : \boldsymbol{R})\boldsymbol{\Psi}(\boldsymbol{r} : \boldsymbol{R}) = \boldsymbol{\Psi}(\boldsymbol{r} : \boldsymbol{R}) \cdot \mathbf{E}(\boldsymbol{R}) \tag{1}$$

provide useful first approximations to the chemical and physical attributes of molecules and other atomic aggregates.[15] Here, the row vector $\boldsymbol{\Psi}(\boldsymbol{r} : \boldsymbol{R})$ contains the desired eigenstates, the diagonal matrix $\mathbf{E}(\boldsymbol{R})$ contains the corresponding energy eigenvalues, $\boldsymbol{r}$ refers to the space and spin coordinates of the n_t electrons of the system, and $\boldsymbol{R}$ designates the fixed positions $(\boldsymbol{R}_1, \boldsymbol{R}_2, \ldots \boldsymbol{R}_N)$ of the N atomic nuclei.

The non-relativistic Hamiltonian operator in Eq. (1),

$$\hat{H}(\boldsymbol{r} : \boldsymbol{R}) = \sum_{k=1}^{n_t} -\frac{\hbar^2}{2m}\nabla_k^2 - \sum_{\alpha=1}^{N}\sum_{k=1}^{n_t}\frac{Z_\alpha e^2}{r_{k\alpha}} + \sum_{k=1}^{n_t-1}\sum_{k'=k+1}^{n_t}\frac{e^2}{r_{kk'}} + \sum_{\alpha=1}^{N-1}\sum_{\beta=\alpha+1}^{N}\frac{Z_\alpha Z_\beta e^2}{R_{\alpha\beta}}, \tag{2}$$

contains the familiar kinetic, electron-nuclear attraction, and electron and nuclear repulsion operators and is totally symmetric in all electron coordinates.[16] Consequently, the solutions of Eq. (1) can be classified according to the irreducible representations of the symmetric group S_{n_t}, with the totally antisymmetric solutions providing the physically significant Schrödinger eigenstates.[17]

The atomic spectral-product representation is written in the outer-product ($\otimes$) form[7−10]

$$\boldsymbol{\Phi}(\boldsymbol{r} : \boldsymbol{R}) = \left\{\boldsymbol{\Phi}^{(1)}(\boldsymbol{1}) \otimes \boldsymbol{\Phi}^{(2)}(\boldsymbol{2}) \otimes \cdots \boldsymbol{\Phi}^{(N)}(\boldsymbol{n})\right\}_O, \tag{3}$$

where the row vectors $\mathbf{\Phi}^{(\alpha)}(\boldsymbol{i})$ contain the orthonormal antisymmetric eigenstates of the constituent atoms ($\alpha = 1$ to N) specified by the quantum numbers $(E, L, M_L, S, M_S, P)_\alpha$,[18] with $\boldsymbol{i}$ referring to the coordinates of the n_α electrons arbitrarily assigned to the atom α measured relative to the atomic centers $\boldsymbol{R}_\alpha$. The subscript "O" in Eq. (3) indicates the adoption of a particular ordering convention for the vector sequence of spectral-product functions employed. More detailed descriptions of these and of the other notational conventions of Eqs. (1) to (3) are reported elsewhere.[7−12]

Although the representation of Eq. (3) is not term-by-term antisymmetric in all electron coordinates, it is, in fact, complete in the limit of spectral closure for representations of totally antisymmetric aggregate eigenstates.[1,19] Accordingly, Eq. (3) is in this connection formally equivalent to the more familiar explicitly (term-by-term) antisymmetric form[6]

$$\begin{aligned} \mathbf{\Phi}_A(\boldsymbol{r} : \boldsymbol{R}) &\equiv \hat{P}_A \mathbf{\Phi}(\boldsymbol{r} : \boldsymbol{R}) \\ &= \hat{P}_A \left\{ \mathbf{\Phi}^{(1)}(\boldsymbol{1}) \otimes \mathbf{\Phi}^{(2)}(\boldsymbol{2}) \otimes \cdots \mathbf{\Phi}^{(N)}(\boldsymbol{n}) \right\}_O , \end{aligned} \tag{4}$$

where

$$\hat{P}_A \equiv (n_t!)^{-1/2} (n_1! n_2! \cdots n_N!)^{-1/2} \sum_{p=1}^{n_t!} (-1)^{\delta_p} \hat{P}_p \tag{5}$$

is the aggregate antisymmetrizer,[17] normalized to insure that $\langle \hat{P}_A \mathbf{\Phi}(\boldsymbol{r} : \boldsymbol{R}) | \hat{P}_A \mathbf{\Phi}(\boldsymbol{r} : \boldsymbol{R}) \rangle \rightarrow \mathbf{I}$ in the limit ($\boldsymbol{R} \rightarrow \boldsymbol{\infty}$), in accordance with the orthonormality of the square-integrable antisymmetric atomic eigenstates in the row vectors $\mathbf{\Phi}^{(\alpha)}(\boldsymbol{i})$. Alternatively, it is possible to enforce aggregate electron antisymmetry employing a coset decomposition of the antisymmetrizer to isolate those electron permutations not completely internal to the already antisymmetric atomic eigenstates.[6,20]

An important difference between the foregoing two representations is found in their respective closure relations. In the case of the orthonormal representation of Eq. (3), the closure expression is $\mathbf{\Phi}(\boldsymbol{r} : \boldsymbol{R}) \cdot \mathbf{\Phi}(\boldsymbol{r}' : \boldsymbol{R})^\dagger = \delta(\boldsymbol{r} - \boldsymbol{r}' : \boldsymbol{R})$, where $\delta(\boldsymbol{r} - \boldsymbol{r}' : \boldsymbol{R})$ applies to all irreducible representations of S_{n_t} spanned by the basis, whereas the closure expression is $\mathbf{\Phi}_A(\boldsymbol{r} : \boldsymbol{R}) \cdot \mathbf{\Phi}_A(\boldsymbol{r} : \boldsymbol{R})^\dagger = Q \delta_A(\boldsymbol{r} - \boldsymbol{r}' : \boldsymbol{R})$ for the non-orthogonal explicitly antisymmetric representation of Eq. (4), where $Q = n_t!/(n_1! n_2! \cdots n_N!)$ is the redundancy of the explicitly antisymmetric basis of Eq. (4) in the closure limit.[10]

B. Hamiltonian Matrices in the Spectral-Product Representations.

It is convenient to rewrite the Hamiltonian operator of Eq. (2) in a form suggested by the arbitrary assignments of electrons to atoms made in Eq. (3) in constructing spectral-product matrix representatives. Specifically, the Hamiltonian operator of Eq. (2) is written

$$\hat{H}(\boldsymbol{r}:\boldsymbol{R}) = \sum_{\alpha=1}^{N} \hat{H}^{(\alpha)}(\boldsymbol{i}) + \sum_{\alpha=1}^{N-1} \sum_{\beta=\alpha+1}^{N} \hat{V}^{(\alpha,\beta)}(\boldsymbol{i};\boldsymbol{j}:\boldsymbol{R}_{\alpha\beta}), \tag{6}$$

where

$$\hat{H}^{(\alpha)}(\boldsymbol{i}) = \sum_{i}^{n_\alpha} \Big\{ -\frac{\hbar^2}{2m}\nabla_i^2 - \frac{Z_\alpha e^2}{r_{i\alpha}} \Big\} + \sum_{i}^{n_\alpha - 1} \sum_{i'=i+1}^{n_\alpha} \frac{e^2}{r_{ii'}} \tag{7}$$

includes the electronic terms arbitrarily associated with the atom α, and

$$\hat{V}^{(\alpha,\beta)}(\boldsymbol{i};\boldsymbol{j}:\boldsymbol{R}_{\alpha\beta}) = \frac{Z_\alpha Z_\beta e^2}{R_{\alpha\beta}} - \sum_{i}^{n_\alpha} \frac{Z_\beta e^2}{r_{i\beta}} - \sum_{j}^{n_\beta} \frac{Z_\alpha e^2}{r_{j\alpha}} + \sum_{i}^{n_\alpha} \sum_{j}^{n_\beta} \frac{e^2}{r_{ij}}, \tag{8}$$

includes the Coulombic interaction terms associated with the pair of atoms (α, β).

Employing the basis sets of Eqs. (3) and (4) in variational solutions of Eq. (1) gives the matrix Schrödinger equations

$$\mathbf{H}(\boldsymbol{R}) \cdot \mathbf{U}_{\mathbf{H}}(\boldsymbol{R}) = \mathbf{U}_{\mathbf{H}}(\boldsymbol{R}) \cdot \mathbf{E}(\boldsymbol{R}), \tag{9}$$

and

$$\mathbf{H}_A(\boldsymbol{R}) \cdot \mathbf{V}_{\mathbf{H}}(\boldsymbol{R}) = \mathbf{S}(\boldsymbol{R}) \cdot \mathbf{V}_{\mathbf{H}}(\boldsymbol{R}) \cdot \mathbf{E}(\boldsymbol{R}), \tag{10}$$

where

$$\mathbf{H}(\boldsymbol{R}) \equiv \langle \boldsymbol{\Phi}(\boldsymbol{r}:\boldsymbol{R}) | \hat{H}(\boldsymbol{r}:\boldsymbol{R}) | \boldsymbol{\Phi}(\boldsymbol{r}:\boldsymbol{R}) \rangle = \sum_{\alpha=1}^{N} \mathbf{H}^{(\alpha)} + \sum_{\alpha=1}^{N-1} \sum_{\beta=\alpha+1}^{N} \mathbf{V}^{(\alpha,\beta)}(\boldsymbol{R}_{\alpha\beta}), \tag{11}$$

and

$$\mathbf{H}_A(\boldsymbol{R}) \equiv \langle \boldsymbol{\Phi}_A(\boldsymbol{r}:\boldsymbol{R}) | \hat{H}(\boldsymbol{r}:\boldsymbol{R}) | \boldsymbol{\Phi}_A(\boldsymbol{r}:\boldsymbol{R}) \rangle = \sum_{\alpha=1}^{N} \mathbf{H}^{(\alpha)}(\boldsymbol{R}) + \sum_{\alpha=1}^{N-1} \sum_{\beta=\alpha+1}^{N} \mathbf{V}^{(\alpha,\beta)}(\boldsymbol{R}), \tag{12}$$

are the respective Hamiltonian matrices.

In Eq. (9), the unitary solution matrix $\mathbf{U_H}(\boldsymbol{R})$ diagonalizes the Hamiltonian matrix of Eq. (11) constructed in the orthonormal basis of Eq. (3). By contrast, the matrix $\mathbf{V_H}(\boldsymbol{R})$ in Eq. (10) is generally not unitary since the metrically-defined Hamiltonian matrix of Eq. (12) is constructed in the non-orthogonal basis of Eq. (4). Rather, $\mathbf{V_H}(\boldsymbol{R})$ satisfies the condition $\mathbf{V_H}(\boldsymbol{R})^\dagger \cdot \mathbf{S}(\boldsymbol{R}) \cdot \mathbf{V_H}(\boldsymbol{R}) = \mathbf{I}$,[15] with the metric matrix $\mathbf{S}(\boldsymbol{R})$ here and in Eq. (10) given by the expression

$$\mathbf{S}(\boldsymbol{R}) \equiv \langle \hat{P}_A \boldsymbol{\Phi}(\boldsymbol{r} : \boldsymbol{R}) | \hat{P}_A \boldsymbol{\Phi}(\boldsymbol{r} : \boldsymbol{R}) \rangle = Q^{1/2} \langle \boldsymbol{\Phi}(\boldsymbol{r} : \boldsymbol{R}) | \hat{P}_A | \boldsymbol{\Phi}(\boldsymbol{r} : \boldsymbol{R}) \rangle, \tag{13}$$

where the factor $Q = n_t!/(n_1!n_2! \cdots n_N!)$ is the aforementioned redundancy of the explicitly antisymmetric basis of Eq. (4) in the closure limit.[10] Evidently, $\mathbf{S}(\boldsymbol{R})$ has an interpretation as the matrix representative of the antisymmetrizer of Eq. (5) in the basis of Eq. (3), separate from its role as the metric matrix of the non-orthogonal basis of Eq. (4).

Although the Hamiltonian matrices of Eqs. (11) and (12) are similar in form, the individual atomic and atomic-pairwise interaction terms shown there differ significantly in the two representations. Specifically, the atomic terms in Eq. (11) obtained from Eq. (7) are independent of atomic position, and the Coulombic interaction terms obtained from Eq. (8) depend only on the vector separation $\boldsymbol{R}_{\alpha\beta}$ of an individual atomic pair (α, β). By contrast, the terms in Eq. (12), which must be evaluated using the Hamiltonian of Eq. (2), formally depend on the positions $\boldsymbol{R}$ of all the atoms in the aggregate due to the overall electron antisymmetry of the basis of Eq. (4). That is, because the electronic coordinates in the representation of Eq. (4) appear at all the atomic centers, the individual Coulombic interactions in the Hamiltonian of Eq. (2) can be alternatively inter- or intra-atomic terms, and the partitioning of Eqs. (6) to (8), which constitutes an assignment of particular electrons to specific atomic centers, can not be employed in this case.

The simpler forms of the terms appearing in Eq. (11) relative to those in Eq. (12) are largely consequences of the orthonormality of the spectral-product basis employed in the absence of prior enforcement of overall aggregate electron antisymmetry, the use of atomic eigenstates in the representation, and the atomic pairwise-additive nature of the interaction terms in the Hamiltonian operator of Eq. (6). By contrast, the atomic-pairwise nature

of the interaction terms in the Hamiltonian operator can not be employed to advantage in conjunction with use of the explicitly antisymmetric representation of Eq. (4). It spite of the apparent differences in the two representations, both can give the same physical Schrödinger eigenstates $\mathbf{\Psi}_p(\boldsymbol{r}:\boldsymbol{R}) = \{\mathbf{\Phi}(\boldsymbol{r}:\boldsymbol{R})\cdot\mathbf{U_H}(\boldsymbol{R})\}_p = \{\mathbf{\Phi}_A(\boldsymbol{r}:\boldsymbol{R})\cdot\mathbf{V_H}(\boldsymbol{R})\}_p$ and energies $\{\mathbf{E}(\boldsymbol{R})\}_{pp}$ under appropriate conditions.

C. Isolation of Physical Eigenstates in the Spectral-Product Representations.

It has been shown that the basis of Eq. (3) spans the totally antisymmetric representation of the aggregate n_t-electron symmetric group S_{n_t} once and only once in the limit of closure, although other unphysical non-totally-antisymmetric (non-Pauli) representations of S_{n_t} are also spanned by the basis.[10] The non-Pauli solutions are accordingly included in the columns of the unitary transformation matrix $\mathbf{U_H}(\boldsymbol{R})$ of Eq. (9). By contrast, although the solutions of Eq. (10) are totally antisymmetric by construction, they generally become unstable in large representations, consequent of the linear dependence arising from the Q-fold redundancy of the basis of Eq. (4) in the closure limit. These two assertions are closely related, and suggest the possible equivalence of results obtained employing either "prior" or "post" antisymmetrization in extracting physically acceptable solutions from the molecular Schrödinger equation in the two representations of Eqs. (3) and (4).

The desired Pauli and linearly-independent solutions can be obtained by transforming Eqs. (9) and (10) to representations which isolate totally antisymmetric and linearly-independent subspaces, respectively, and can be shown to be equivalent in the limit of spectral closure. The unitary transformation matrix $\mathbf{U_S}(\boldsymbol{R})$ required to accomplish this partitioning of Eqs. (9) and (10) is obtained from diagonalization

$$\mathbf{U_S}(\boldsymbol{R})^\dagger\cdot\mathbf{S}(\boldsymbol{R})\cdot\mathbf{U_S}(\boldsymbol{R}) = \mathbf{s}_d(\boldsymbol{R}) = \begin{pmatrix} \{\mathbf{s}_d(\boldsymbol{R})\}_{pp} & \mathbf{0} \\ \mathbf{0} & \{\mathbf{s}_d(\boldsymbol{R})\}_{uu} \end{pmatrix} \rightarrow \begin{pmatrix} Q\mathbf{I}_{pp} & \mathbf{0} \\ \mathbf{0} & \mathbf{0} \end{pmatrix} \qquad (14)$$

of the Hermitian metric matrix of Eq. (13). Here, the non-negative eigenvalue matrix $\mathbf{s}_d(\boldsymbol{R})$ is partitioned into an upper diagonal $\{\mathbf{s}_d(\boldsymbol{R})\}_{pp}$ containing the largest eigenvalues ordered in decreasing value, which tend to the indicated common redundancy factor Q in the closure limit, and a lower diagonal $\{\mathbf{s}_d(\boldsymbol{R})\}_{uu}$ of eigenvalues which tend to zero in this

limit, so ordered by appropriate arrangement of the columns of the transformation matrix $\mathbf{U_S}(\boldsymbol{R})$ into physical (p) and unphysical (u) blocks.

The diagonalization of Eq. (14) is seen to correspond to construction of eigenstates of the Hermitian antisymmetrizer in the spectral-product basis of Eq. (3) in the form

$$\mathbf{\Phi_S}(\boldsymbol{r}:\boldsymbol{R}) \equiv \mathbf{\Phi}(\boldsymbol{r}:\boldsymbol{R}) \cdot \mathbf{U_S}(\boldsymbol{R}) \rightarrow \big\{\{\mathbf{\Phi_S}(\boldsymbol{r}:\boldsymbol{R})\}_p, \{\mathbf{\Phi_S}(\boldsymbol{r}:\boldsymbol{R})\}_u\big\}, \tag{15}$$

where $\{\mathbf{\Phi_S}(\boldsymbol{r}:\boldsymbol{R})\}_p$ contains totally antisymmetric states corresponding to the non-zero eigenvalues of the antisymmetrizer, and $\{\mathbf{\Phi_S}(\boldsymbol{r}:\boldsymbol{R})\}_u$ contains non-Pauli states corresponding to the zero eigenvalues of the antisymmetrizer in the closure limit. By contrast, in the explicitly, or term-by-term, antisymmetric basis of Eq. (4), the states generated by the transformation of Eq. (14) are written in the canonically orthogonalized form

$$\mathbf{\Phi_S}(\boldsymbol{r}:\boldsymbol{R}) \equiv \mathbf{\Phi}_A(\boldsymbol{r}:\boldsymbol{R}) \cdot \mathbf{U_S}(\boldsymbol{R}) \cdot \mathbf{s}_d(\boldsymbol{R})^{-1/2} \rightarrow \big\{\{\mathbf{\Phi_S}(\boldsymbol{r}:\boldsymbol{R})\}_p, \{\mathbf{\Phi_S}(\boldsymbol{r}:\boldsymbol{R})\}_u \rightarrow \mathbf{0}\big\}, \tag{16}$$

which are correctly normalized linearly-independent combinations of the original basis and un-normalizable null states associated with linearly-dependent combinations of the basis of Eq. (4).[21] In the case of degenerate eigenvalues, the eigenstates of Eqs. (15) and (16) are generally arbitrary but are nevertheless separated into invariant subspaces. Of course, in the large-separation limit $\mathbf{S}(\boldsymbol{R} \rightarrow \boldsymbol{\infty}) \rightarrow \mathbf{I}$, in which case the eigenvalues of the metric matrix are all unity, both representations of Eqs. (3) and (4) are orthonormal and the states of Eqs. (15) and (16) are not required.

Equations (14) and (15) indicate that the spectrum of $\hat{P}_A$ acting in the domain of the spectral-product basis of Eq. (3) is that of a compact Hermitian operator,[22] with zero providing a lower limiting point of accumulation of the spectrum and the associated non-Pauli states $\{\mathbf{\Phi_S}(\boldsymbol{r}:\boldsymbol{R})\}_u$ of Eq. (15) corresponding to its null space $\hat{P}_A\{\mathbf{\Phi_S}(\boldsymbol{r}:\boldsymbol{R})\}_u \rightarrow \mathbf{0}$. The states $\{\mathbf{\Phi_S}(\boldsymbol{r}:\boldsymbol{R})\}_p$ of Eq. (15) are associated with the upper limiting point, $\hat{P}_A\{\mathbf{\Phi_S}(\boldsymbol{r}:\boldsymbol{R})\}_p \rightarrow Q^{1/2}\{\mathbf{\Phi_S}(\boldsymbol{r}:\boldsymbol{R})\}_p$, and correspond to the physically significant totally antisymmetric spectrum of the antisymmetrizer. The linearly-independent combinations of the term-by-term antisymmetric basis functions of Eq. (4) given by Eq. (16) are identical to the totally antisymmetric states of Eq. (15) in the closure limit,[10] whereas the linearly-dependent states of Eq. (16) are seen to be eliminated by the development.[21]

The physically significant blocks of the Hamiltonian matrices of Eqs. (11) and (12) are obtained from the matrix $\mathbf{U_S}(\boldsymbol{R})$ in the upper left-hand forms

$$\{\mathbf{H}(\boldsymbol{R})\}_{pp} \equiv \{\mathbf{U_S}(\boldsymbol{R})^{\dagger} \cdot \mathbf{H}(\boldsymbol{R}) \cdot \mathbf{U_S}(\boldsymbol{R})\}_{pp} \tag{17}$$

$$\{\mathbf{H}_A(\boldsymbol{R})\}_{pp} \equiv \{\mathbf{s}_d(\boldsymbol{R})^{-1/2}\}_{pp} \cdot \{\mathbf{U_S}(\boldsymbol{R})^{\dagger} \cdot \mathbf{H}_A(\boldsymbol{R}) \cdot \mathbf{U_S}(\boldsymbol{R})\}_{pp} \cdot \{\mathbf{s}_d(\boldsymbol{R})^{-1/2}\}_{pp}, \tag{18}$$

where now all terms in both Hamiltonian matrices depend formally on the positions $\boldsymbol{R}$ of all the atoms in the aggregate. The unitary transformation matrix $\mathbf{U_S}(\boldsymbol{R})$ of Eq. (14) obtained from the metric matrix of Eq. (13) is seen to be responsible for incorporating the non-local effects of inter-atomic aggregate electron permutation symmetry in the Hamiltonian matrix of Eq. (11) by virtue of Eq. (17). Overall electron antisymmetry can be enforced as required in this approach in accordance with the spatial separations of the individual atoms and the perceived strengths of their interactions in the Hamiltonian of Eq. (17), rather than as a possibly encumbering overall global constraint, as employed in the Hamiltonian matrix in Eq. (18). Although the role of the transformation matrix $\mathbf{U_S}(\boldsymbol{R})$ in the explicitly antisymmetric representation of Eq. (4) is to isolate the linearly-independent subspace present therein, it would seem useful to also employ approximation methods in its evaluation in certain cases, although the more significant advantage of this approach is expected to be found in connection with Eq. (17).

Finally, identical physically significant Schrödinger eigenstates are obtained from the immediately foregoing Hamiltonian matrices in the form $\boldsymbol{\Psi}_p(\boldsymbol{r} : \boldsymbol{R}) = \{\boldsymbol{\Phi}(\boldsymbol{r} : \boldsymbol{R})\}_p \cdot \{\mathbf{U_H}(\boldsymbol{R})\}_{pp}$, where $\{\boldsymbol{\Phi}(\boldsymbol{r} : \boldsymbol{R})\}_p$ is obtained from either Eq. (15) or (16) and $\{\mathbf{U_H}(\boldsymbol{R})\}_{pp}$ is obtained from either of the Hamiltonian matrices of Eqs. (17) or (18). Although the requirements of computational implementations of the two approaches differ significantly, in view of the "post" and "prior" incorporation of aggregate electron antisymmetry in the two Hamiltonian matrices, the developments are clearly united through use of the metric matrix of Eq. (13) in isolating a common invariant physical subspace in which to construct Schrödinger eigensolutions.

III. Computational Implementations and Applications

Algorithms and computer codes have been devised to evaluate the various expressions given in the preceding Sections. In brief, a valence-bond code suite (CRUNCH[23]) has been modified to accommodate molecular integrals evaluated in real Slater orbitals (SMILES[24]), and transformations devised from the standard tableau descriptions of configurational state functions and Hamiltonian and metric matrix elements of the valence-bond formalism to the atomic spectral-product expressions. Computational results obtained in this way are reported in Section **A** for H_2 and H_3 molecules, in Section **B** for diatomic CH, and in Section **C** for triatomic CH_2. These calculations are illustrative of selected aspects of the approach, and of the capabilities of the computational algorithms and codes devised, and are not meant to provide exhaustive computational descriptions of the quantities reported.

A. Diatomic and Triatomic Hydrogen Molecules.

Although the metric matrix is familiar in connection with canonical transformations of one-electron orbital basis sets,[21] its attributes and importance in connection with many-electron basis states are perhaps less familiar, particularly in the context of the spectral-product representations described here. Of particular interest is the function of the metric matrix in providing a measure of the spectral closure of the representation of Eq. (3) in the absence of explicit antisymmetry and of the redundancy of the representation of Eq. (4), particularly in connection with commonly employed ionic terms involving the transfer of one or more electrons from one atom to others. Illustrative molecular calculations involving hydrogen atoms help to clarify these issues, and demonstrate the capabilities of the algorithms and codes devised.

In Figure 1 are shown the eigenvalues of the metric matrix of Eq. (13) for symmetric collinear H_3 as a function of atomic separation ($R_{ab} = R_{bc}$), constructed in (a) $2s1p$ and (b) $3s2p$ atomic Slater basis sets employing hydrogenic exponents. These atomic orbitals give representations $\mathbf{\Phi}^{(H_3)}(\boldsymbol{r} : \boldsymbol{R}) = \left\{\mathbf{\Phi}^{(H_a)}(\mathbf{1}) \otimes \mathbf{\Phi}^{(H_b)}(\mathbf{2}) \otimes \mathbf{\Phi}^{(H_c)}(\mathbf{3})\right\}_O$ which include 375 and 2187 terms, respectively. The eigenvalues of the antisymmetrizer of Eq. (5) in these representations are seen to appear only in the allowable interval $(0,Q)$ where

$Q = 3!/(1!1!1!)$=6, and to fill the interval for smaller values of atomic separation. The great many values near 0 in Panel (b) are in accordance with the lower end of the spectrum of $\hat{P}_A$ providing a point of accumulation. The eigenstates corresponding to these approximately zero eigenvalues refer to non-totally antisymmetric states in the product basis [Eqs. (3) and (15)], whereas in the prior antisymmetrized basis they refer to linearly-dependent states [Eqs. (4) and (16)]. Conversely, the states of Eqs. (15) and (16) corresponding to the largest eigenvalues of Figure 1 refer to approximately totally antisymmetric and linearly-independent states, respectively. Note that the value Q=6 implies the antisymmetric basis of Eq. (4) is six-fold redundant in the limit of closure in this case, which redundancy is removed by the canonical orthogonalization procedure of Eq. (16). As the number of basis functions and their spatial extent are increased, the eigenvalues of Figure 1 converge to the upper and lower limiting points of the spectrum for finite values of atomic separation, whereas they approach unity in the limit of large separation in any square-integrable representation.

Although large orbital basis sets are generally required to achieve convergence in spectral-product representation, metric matrices constructed even in small basis sets provide useful information. In Figure 2 are shown constant-value contours for the two doublet eigenvalues of the metric matrix for T-shaped H_3 as functions of width (w) and height (h) obtained in a minimal $1s^3$ spectral-product representation. In panel (a), the contours are monotonically increasing from that labeled 1.0, whereas in panel (b) they are monotonically decreasing from that labeled 0.9. The cusps in the contours of both panels indicate the presence of a seam of intersection in the two surfaces along the $w = 1.155\ h$ line corresponding to D_{3h} symmetry. This high-symmetry seam corresponds to the better-known seam of intersection of the two lowest-lying doublet energy surfaces in H_3,[25] identified here entirely on basis of the eigenvalues of the metric matrix in the absence of energy calculations. Such calculations of metric matrices, which entail evaluations only of overlap matrix elements, can provide useful information in other molecular cases more generally.

The spectral product representation of Eq. (3) is complete employing only the indicated neutral atomic states, and the associated antisymmetrized basis of Eq. (4) is correspond-

ingly Q-fold redundant in the closure limit. It is instructive, however, to examine the effects of adding commonly employed ionic or charge-transfer configurations to the basis. In Figure 3 are shown the singlet and triplet eigenvalues of the metric matrix of Eq. (13) for diatomic hydrogen constructed in a $7s5p3d2f1g$ Slater basis set employing fixed hydrogen $1s, 2p, 3d, 4f, 5g$ exponents in Sturmian sequences.[26] The eigenvalues shown correspond to single-excitation configuration-interaction calculations, including both covalent (H-H - 119 terms) and ionic (H^+H^- and H^+H^- - 154 terms) structures. Although the redundancy factor is $Q = 2!/(1!1!)$=2 for the spectral-product or covalent representations of Eqs. (3) and (4) in this case, the presence of the additional charge-transfer terms gives rise to eigenvalues which appear in the larger interval (0,4). This is a consequence of the four-fold redundancy of the combined covalent and ionic basis employed in the calculations of Figure 3 in the closure limit. Specifically, the band of near zero eigenvalues in Figure 3 arises from the near linear-dependence of charge-transfer terms with the diffuse covalent excitations - this band is absent in the eigenvalue spectrum (0,2) obtained with covalent terms alone.[9,10] Moreover, the bands of eigenvalues approaching 2 for larger separation are also consequences of the charge-transfer terms, which continue to provide a two-fold redundant explicitly antisymmetric representation in this limit, whereas the bands of eigenvalues approaching unity at large separation arise from the covalent structures in the representation. The results of Figure 3 suggest the eigenvalues of the metric matrix can distinguish among the types of structures present in the representation employed, largely confirm the redundancy of covalent and ionic terms commonly employed in molecular calculations, and emphasize the importance of removing these redundancies in large-basis-set calculations.

Illustrations of the capabilities of the Slater-based spectral-product codes devised for energy calculations are given in Figures 4 and 5, which depict low-lying (n=1 and 2) H_2 singlet and triplet potential energy curves, respectively, obtained from full configuration-interaction calculations in an optimal $5s3p2d1f$ valence Slater basis.[27] These results are in general but not precise accord with the most accurate previous calculations available for the indicated states.[28] Of particular interest are the shapes of the $B^1\Sigma_u^+$ and E,$F^1\Sigma_g^+$ curves, the presence of a double well in the latter curve and in the G,$K^1\Sigma_g^+$ curve, and the large barrier in the f $^3\Pi_u$ state. The long-range nature of the $B^1\Sigma_u^+$ and E,$F^1\Sigma_g^+$ curves, which provide

good approximations to the accurate values, is commonly but subjectively attributed to contributions from charge-transfer terms. The calculated G,K $^1\Sigma_g^+$ and f $^3\Pi_u$ curves provide reasonably quantitative descriptions of the known detailed shapes of these two curves, but are not in precise agreement with the results of highly accurate calculations.[28] Of course, highly accurate calculation of the excited-state potential energy curves of H_2 are generally performed employing special basis sets on a state-by-state basis. It is therefore satisfying that the results of Figures 4 and 5 are obtained from single diagonalizations of matrices constructed in Slater-based spectral-product representations, which methodology is applicable to other molecules more generally.

B. Diatomic CH Molecule.

The foregoing spectral-product representations of molecules containing hydrogen atoms (H_2, H_3) are closely related to corresponding valence-bond descriptions, the two approaches differing largely in the normalization conventions employed for orbital-product states, and a pre-diagonalization of the atomic hydrogen Hamiltonian in the spectral-product development. The situation is quite different for molecules containing many-electron atoms. The differences between metric or Hamiltonian matrices constructed in valence-bond and spectral-product representation can be illustrated in these cases employing the well-studied diatomic CH molecule as a simple example. In this example, both valence-bond and spectral-product metric and Hamiltonian matrices are constructed employing identical hydrogen atom $1s$ spin orbitals and $1s^2(2s^22p^2 + 2s2p^3 + 2p^4)$ carbon atom valence-shell configurations, the latter giving rise to fifty-five distinct atomic multiplet states. The valence-bond states made from these orbital configurations are in the forms of standard tableau functions which are employed directly in constructing the required matrices,[23] whereas in the spectral-product representation the hydrogen atom $^2S^e$ and carbon atom [$(2)^3P^e$, $(2)^1D^e$, $(2)^1S^e$, $^5S^o$, $^3D^o$, $^3P^o$, $^1D^o$, $^3S^o$, $^1P^o$] multiplet states are constructed and the spectral-product matrices of Eqs. (11) to (13) are evaluated employing algorithms and codes devised explicitly for this purpose. Specifically, the expression $\mathbf{\Phi}_{sp}^{(CH)}(\boldsymbol{r} : R) = \mathbf{\Phi}_{vb}^{(CH)}(\boldsymbol{r} : R) \cdot \mathbf{V}^{(CH)}(R)$ is employed to affect the basis transformation, where $\mathbf{V}^{(CH)}(R)$ is a non-unitary matrix constructed from an ordered product of corre-

sponding atomic H and C transformation matrices. This $vb \rightarrow sp$ transformation approach is employed in constructions of the metric and Hamiltonian matrices in the spectral-product representation from their forms calculated in the valence-bond representation.

In Figure 6 are shown eigenvalues of the doublet- and quartet-state metric matrix for diatomic CH constructed in the aforementioned atomic valence configurations using an optimized valence orbital basis.[27] The solid lines refer to eigenvalues of the matrix in the orthonormal spectral-product representation of Eq. (3), whereas the dashed lines are those obtained in the same configurational basis employing the standard tableau functions of valence-bond theory.[23] The two sets of eigenvalues of Figure 6 are evidently quite different, those in the valence-bond description grouping in accordance with the normalizations of standard tableau functions transforming under particular irreducible representations of S_{n_t} and approaching different limits at large atomic separation. By contrast, there are only three distinct highly degenerate eigenvalues of the spectral-product metric matrix in Figure 6, which are seen to approach unity in accordance with the orthonormality of the spectral-product representation. The small number of distinct eigenvalues of the latter representation relates to use of only $n = 1$ shell hydrogen and n=2 shell carbon multiplet configurations in the calculations and to the orthogonality of the representation. Relatedly, although the allowable eigenvalue interval for CH is formally Q=7!/(6!1!1!)=7, the representation employed in Figure 6 is too small to exhibit the full redundancy of the basis of Eq. (4) in this case.

Just as the metric matrices obtained in the valence-bond and spectral-product representations generally differ, so also do the corresponding Hamiltonian matrices. Nevertheless, the energy eigenvalues obtained from the two representations employing identical atomic configurations must be identical, providing a useful test of the algorithms and codes devised to perform the present calculations. In Figure 7 are shown low-lying potential energy curves for CH obtained in $(1s)^2\mathrm{S}^e$ atomic hydrogen and $(1s^2 2s^2 2p^2)[^3\mathrm{P}^e, ^1\mathrm{D}^e, ^1\mathrm{S}^e]$ atomic carbon representations. The two sets of potential energy curves obtained from the valence-bond and spectral-product representations are found to be identical, but to provide very poor representations of the known accurate values.[13] Specifically, although the ground state is

correctly predicted to be of $^2\Pi$ symmetry, the calculated chemical binding energy is much too small, the predicted $A^2\Delta$ state falls above the $B^2\Sigma^-$ state, and no other chemically bound states are predicted by the representation.

In Figure 8 are shown the results of calculations similar to those of Figure 7, now including the additional atomic carbon n=2 shell multiplet configurations $1s^2 2s 2p^3$ and $1s^2 2p^4$. The former configuration gives rise to the important $^5S^o$ and $^3D^o$ atomic carbon states which are seen to have significant effect on the calculated potential energy curves. In particular, the $a^4\Sigma^-$, $A^2\Delta$, $B^2\Sigma^-$, and $C^2\Sigma^+$ state curves are significantly lower and in the accepted order, a bound $a^4\Sigma^-$ curve is now obtained, and the ground $X^2\Pi$ state is also more strongly bound. The dramatic lowering of the $a^4\Sigma^-$ state curve is due to the additional $^4\Sigma^-$ configurational state function arising from the atomic carbon $1s^2 2s 2p^3$ valence configuration, which is spectrally concentrated in and dissociates to the $^5S^o$ atomic carbon state, whereas the significant lowering of the $A^2\Delta$ and $B^2\Sigma^-$ state curves correlating with the excited $^1D^e$ atomic carbon state is due to contributions in the spectral-product representation from the high-lying $(1s^2 2s 2p^3)^3D^o$ atomic carbon state. Although population analysis can also be employed to identify the presence of important configurations in calculated wave functions, the atomic spectral concentration of particular atomic components in the representation is particularly meaningful in that these states have physical significance, and are not subjectively based on particular choices of basis sets, methods of calculation, or analysis techniques. Moreover, the contributions from particular atomic-state products are read off directly from the eigenvectors obtained in the representational basis without further manipulations.

C. Triatomic CH_2 Molecule.

The methylene molecule has played an important role in the development of accurate quantum chemical methodologies,[14] and is relevant in connection with the metric matrices and atomic spectral compositions of molecular wave functions of interest here. Calculations similar to those reported above for the CH molecule help to further clarify aspects of these issues, employing atomic multiplet configurational models for illustrative purposes.

In Figure 9 are shown metric matrix eigenvalues in both valence-bond and spectral-product representations employing the hydrogen atom $1s$ and carbon atom $1s^2(2s^22p^2+2s2p^3+2p^4)$ configurations described in the preceding Section. In this case, the redundancy factor for the corresponding basis of Eq. (4) is $Q = 8!/(6!1!1!) = 56$, although the closed $1s^2$ carbon and $1s$ hydrogen shells, and the absence of higher orbital excitations, limits the calculated eigenvalues to a much smaller spectral interval. As in Figure 6 for the CH molecule, the eigenvalues of Figure 9 are very different in the two representations, with the degenerate spectral-product values uniformly approaching unity at large atomic separation and those in the valence-bond representation forming distinct groups associated with the normalizations of standard tableau functions transforming under the different irreducible representations of S_{n_t}. Of course, the corresponding Hamiltonian matrices in the two representations also differ, although the energy eigenvalues must be identical when the same orbital configurations are employed in the two developments.

In Figures 10 and 11 are shown triplet- and singlet-state potential energy curves for methylene in symmetric collinear (H-C-H) arrangements obtained in the multiplet carbon ($1s^22s^22p^2$) and hydrogen ($1s$) atomic configurations employed in the foregoing. The lowest-lying potential curves in this minimal valence multiplet representation are seen to be very weakly bound $^3\Pi_g$ and $^1\Pi_g$ states, whereas the correct lowest-energy triplet and singlet states in symmetric collinear CH_2 arrangement are known to be the $X^3\Sigma_g^-$ and $a^1\Delta_g$ states.[14] Additionally, all other curves in Figures 10 and 11 are seen to be strongly non-bonding. Clearly, the minimal multiplet representation fails to provide even qualitatively correct descriptions of the potential energy curves in CH_2.

In Figures 12 and 13 are shown potential energy curves for the states of Figures 10 and 11, now constructed employing the full carbon atom $1s^2(2s^22p^2 + 2s2p^3 + 2p^4)$ valence-shell configurations also employed in the preceding CH molecule calculations. As in the case of CH, there are dramatic changes in the CH_2 potential curves of Figures 12 and 13 relative to those of Figures 10 and 11. Specifically, the $X^3\Sigma_g^-$ state is seen to become the lowest energy state, the $a^1\Delta_g$ states becomes the lowest-lying single state, and the $c^1\Sigma_g^+$ state becomes the first excited singlet, in accord with the results of accurate calculations.[14] The lowering

of the $X^3\Sigma_g^-$ potential curve is a consequence of the additional $^3\Sigma_g^-$ configuration arising from the presence of the $^5S^o$ carbon atom state in the larger representation, whereas the lowering of the $a^1\Delta_g$ and $c^1\Sigma_g^+$ states is due to molecular states associated with the high-lying $^3D^o$ carbon atom state in the larger atomic representation employed. These assertions are based on examinations of the eigenvectors of the corresponding states, emphasizing the convenience of the atomic spectral-product representation for chemical diagnostic purposes.

IV. Discussion and Concluding Remarks

The spectral-product approach to *ab initio* molecular electronic structure calculations would seem to provide a fresh perspective of sufficient promise to warrant further effort in its computational implementation. The theoretical development presented in Section II is largely pedestrian in nature, but demonstrates rigorously the formal equivalence between enforcement of electron antisymmetry prior to or subsequent to Hamiltonian matrix evaluation in the atomic spectral-product representation. In the case of prior enforcement, the totally antisymmetric but redundant representation employed gives rise to Hamiltonian matrix elements each of which formally depends on the positions of all the atoms in the aggregate, requiring repeated evaluations of such matrix elements in construction of potential energy surfaces. Moreover, the linearly-independent subspace of this redundant representation must be isolated to avoid encountering computational instabilities in obtaining molecular energy eigenfunctions and eigenvalues. By contrast, the post-antisymmerization approach employs a complete but not over-complete representation which gives rise to Hamiltonian matrix elements which can potentially be evaluated once and for all and retained for repeated polyatomic applications. There remains the task in this approach of isolating the totally antisymmeric subspace of the spectral-product representation to obtain the physically significant molecular eigenstates.

The matrix representing the total antisymmetrizer in the spectral-product basis, which is seen from the development of Section II to be equivalent to the metric matrix of its antisymmetrized form, provides a method for isolating the totally antisymmetric subspace of the spectral-product representation, as well as the linearly-independent subspace of its antisymmetric form, by unitary transformation of the Hamiltonian matrix. This unitary-

transformation approach to antisymmetrization provides an alternative to prior global antisymmetrization which need not entail direct diagonalization of the complete aggregate metric matrix. Rather, alternatives can be devised to distinguish among atomic interactions for which antisymmetry is strictly required and those interactions for which it is not required. Since only overlap integrals are needed in evaluations of the metric matrix, with one- and two-electron energy integrals not needed for this purpose, there is considerable opportunity to develop approximation methods which can take advantage of the atomic pairwise-interaction nature of the aggregate Hamiltonian matrix.

The computational applications to simple molecules (H_2, H_3, CH, CH_2) reported in Section III illustrate the role of the eigenvalue spectrum of the metric matrix in simple diatomic and polyatomic cases in assessing closure in the spectral-product representation, and in correspondingly identifying redundancy in its explicitly antisymmetrized form. The allowable range of the eigenvalue spectrum in the spectral-product basis $[0, Q = n_t!/(n_1!n_2!\cdots n_N!)]$ is seen to be determined by the number of electrons in each atom and the total sum of these in the particular normalization of the antisymmetrizer employed. Convergence of the eigenvalues to the extreme points of the allowable range (0 and Q), in accordance with the compact-operator nature of the total antisymmetrizer, corresponds to the separation of totally antisymmetric and non-totally antisymmetric states in the spectral-product basis, or, equivalently, to the separation of linearly-independent and linearly-dependent states in its antisymmetrized form. The introduction of additional terms in the representation, particularly of the charge-transfer terms commonly employed in molecular calculations, is seen to disrupt this simple picture, and to extend the allowable range of the eigenvalue spectrum to accommodate the additional basis-set redundancy introduced. It seems clear that the metric matrix provides a device for developing suitable atomic spectral-product representations entirely in the absence of the molecular electronic energy calculations commonly employed in devising orbital basis sets for use in more conventional calculations.

The illustrative molecular energy calculations reported in Section III do not provide definitive quantitative results for the simple molecules studied (H_2, CH, CH_2), but rather demonstrate to some degree the capabilities of the valence-bond- and Slater-orbital-based algo-

rithms and codes devised for this purpose, as well as the nature of the descriptor of molecular electronic structures the development provides. Calculations of the twelve excited-state potential energy curves in H_2 dissociating to the $n = 2$ atomic limit, obtained from straightforward diagonalizations of singlet and triplet full configuration-interaction energy matrices constructed with standard Slater-orbital basis sets, are found to be in good accord with the most accurate calculations available, as obtained largely but not entirely from a series of individual calculations performed with special basis sets not applicable to other molecules more generally. Additionally, the important role of the $2s2p^3$ configuration in atomic carbon is understood from the new atomic spectral-composition perspective provided by the spectral-product development. Specifcally, the contributions to molecular CH and CH_2 eigenstates from $^5S^0$ and $^3D^0$ atomic carbon states which arise specifically from the $2s2p^3$ configuration are seen to have significant qualitative and quantitative effects on the positions and shapes of selected potential energy curves. Whereas descriptions of such effects in terms of orbital configurations are clearly subjective, the perspective provided by the spectral compositions of molecular electronic wave functions in the spectral-product representation is not, and involves the physically significant many-electron atomic eigenstates of the bonding atoms. It would seem the spectral-product representation provides both a conceptual and a computational basis for studies of molecular electronic eigenstates.

Additional calculations not reported here involving H, C, N, and O atom-containing compounds largely support and amplify the foregoing general conclusions. Studies in progress are now focused on development of signifcantly more efficient and robust computational methods for performing spectral-product calculations, use of larger Slater-orbital representations, and novel means of isolating the required invariant totally antisymmetric subspaces. Progress in these areas will be reported elsewhere in due course.

Acknowledgment.

The financial support of the Air Force Research Laboratory is gratefully acknowledged. We thank Drs. J.A. Sheehy and S.L. Elbert for assistance and advice during the early stages of the investigation, and Professor J.A. McCammon for his kind hospitality and support throughout.

References

[1] Eisenschitz, H.; London, F. *Z. Physik* **1930**, *60*, 491-527.

[2] Hund, F. *Z. Physik* **1927**, *40*, 742-764.

[3] Mulliken, R. *Phys. Rev.* **1928**, *32*, 186-222.

[4] Pauling, L. *PNAS* **1928**, *14*, 359-362.

[5] Slater, J.C. *Phys. Rev.* **1931**, *38*, 1109-1144.

[6] Moffitt, W. *Proc. Roy. Soc. (Lond.) A* **1951**, *210*, 245-268.

[7] Langhoff, P.W.; Hinde, R.J.; Boatz, J.A.; Sheehy, J.A. *Chem. Phys. Lett.* **2002**, *358*, 231-236.

[8] Langhoff, P.W.; Boatz, J.A.; Hinde, R.J.; Sheehy, J.A. in *Low-Lying Potential Energy Surface*, Hoffmann, M.R.; Dyall, K.G. Eds., ACS Symposium Series 828: Washington, DC, USA, 2002; Chapter 10, pp. 221-237.

[9] Langhoff, P.W.; Boatz, J.A.; Hinde, R.J.; Sheehy, J.A. in *Fundamental World of Quantum Chemistry: A Tribute to the Memory of Per-Olov Löwdin*, Brändas, E.; Kryachko, E.S. Eds., Kluwer Academic: Dordrecht, Nederlands, 2004; Volume 3, pp. 97-114.

[10] Langhoff, P.W.; Boatz, J.A.; Hinde, R.J.; Sheehy J.A. *J. Chem. Phys.* **2004**, *121*, 9323-9342.

[11] Langhoff, P.W.; Boatz, J.A.; Hinde, R.J.; Sheehy J.A. *Theor. Chem. Accounts* **2008**, *120*, 199-213.

[12] Langhoff, P.W. *J. Phys. Chem.* **1996**, *100*, 2974-2984.

[13] Kalemos, A.; Mavridis, A.; Metropoulos, A. *J. Chem. Phys.*, **1999**, *111*, 9536-9548.

[14] Kalemos, K.; Dunning, Jr.; T.H., Mavridis, A.; Harrison, J.F. *Can. J. Chem.*, **2004**, *82*, 684-693.

[15] McWeeny, R. *Methods of Molecular Quantum Mechanics*, Academic: London, U.K., 1989; 2^{nd} Edition.

[16] Bethe, H.A.; Salpeter, E.E. *Quantum Mechanics of One- and Two-Electron Atoms*, Springer-Verlag: Berlin, DE, 1957.

[17] Hamermesh, M. *Group Theory*, Addison-Wesley: Reading, Massachusetts, USA, 1962.

[18] Condon, E.U.; Shortley, G.H. *The Theory of Atomic Spectra*, University Press: Cambridge, U.K., 1963.

[19] Courant, R.; Hilbert, D. *Methods of Mathematical Physics*, Interscience: New York, USA, 1966, Volume I, Chapter II.

[20] Chisholm, C.D.H. *Group Theoretical Techniques in Quantum Chemistry*, Academic Press: London, U.K., 1976, Chapter 6.

[21] Szabo, A.; Ostlund, N.S. *Modern Quantum Chemistry: Introduction to Advanced Electronic Structure Theory*, MacMillan: London, U.K., 1982, Chapter 6.

[22] Akhiezer, N.I.; Glazman, I.M. *Theory of Linear Operators in Hilbert Space*, Ungar: New York, USA, 1961, Vol. I.

[23] Gallup, G.A. *Valence Bond Methods: Theory and Applications*, Cambridge University Press: New York, USA, 2002.

[24] Fernádez Rico, J.; Lopez, R.; Ema, I.; Ramírez, G. *J. Comp. Chem.* **2004**, *25*, 1987-1994.

[25] Porter, R.N.; Karplus, M. *J. Chem. Phys.*, **1964**, *40*, 1105-1115.

[26] Shull, H.; and Löwdin, P.-O. *J. Chem. Phys.*, **1955**, *23*, 1362.

[27] Ema, I.; Garcia de la Vega, J.M.; Ramírez, G.; López,; Fernádez Rico, R.J.; Meissner, H.; Paldus, J. *J. Comp. Chem.* **2003**, *24*, 859-868.

[28] Fantz, U.; Wunderlich, D. *Franck-Condon Factors, Transition Probabilities and Radiative Lifetimes for Hydrogen Molecules and Their Isotopomeres*, Report INDC(NDS)-457, International Atomic Energy Agency: Vienna, Austria, 2004.

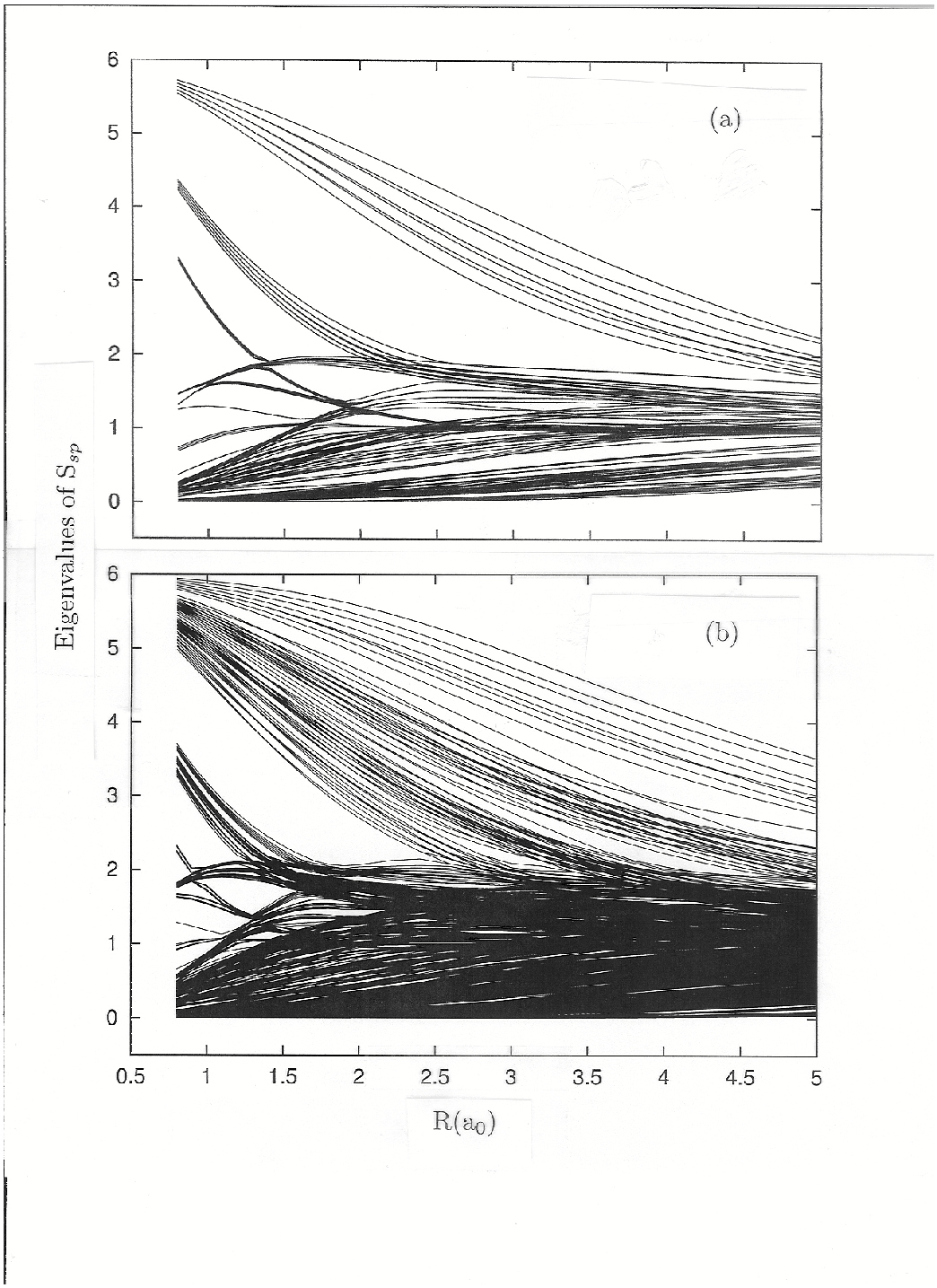

Figure 1. Eigenvalues of the doublet-state metric matrix of Eq. (13) for symmetric ($R_{ab} = R_{bc}$) collinear H_3 as functions of atomic separation (H_a-H_b-H_c): Panel (a) $2s1p$ atomic basis (375 terms); Panel (b) $3s2p$ atomic basis (2187 terms). The limiting points of the spectra are 0 and $Q = 3!/(1!1!1!) = 6$, specifying the redundancy of the basis of Eq. (4) in this case.

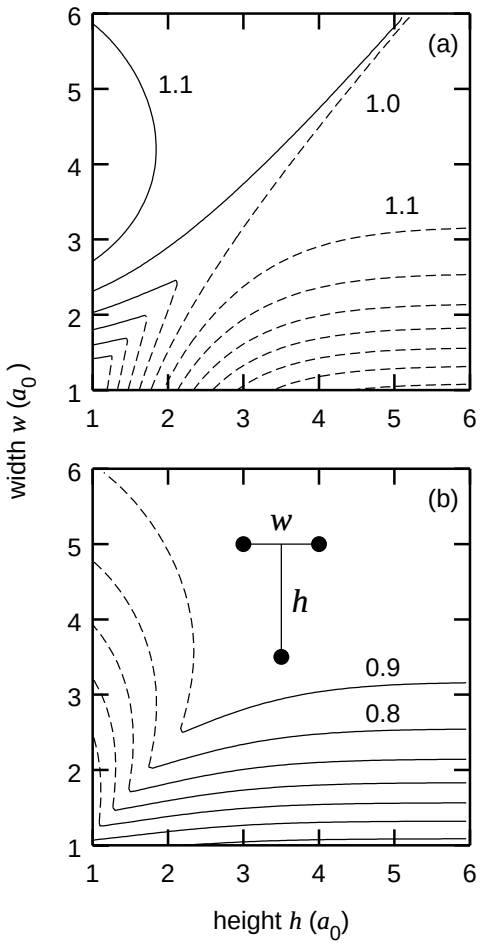

Figure 2. Constant-value contours for the two doublet eigenvalue surfaces of the metric matrix of Eq. (13) for T-shaped arrangements in H_3 constructed in a minimal $1s^3$ representation. Panel (a) - solid lines give the upper surface; Panel (b) - solid lines give the lower surface, employing increments/decrements of 0.1 between adjacent contours in each case. The cusps in the contours of both panels indicate the presence of the seam of crossing of the two surfaces along the $w = 1.155\ h$ line, corresponding to D_{3h} symmetry.[25]

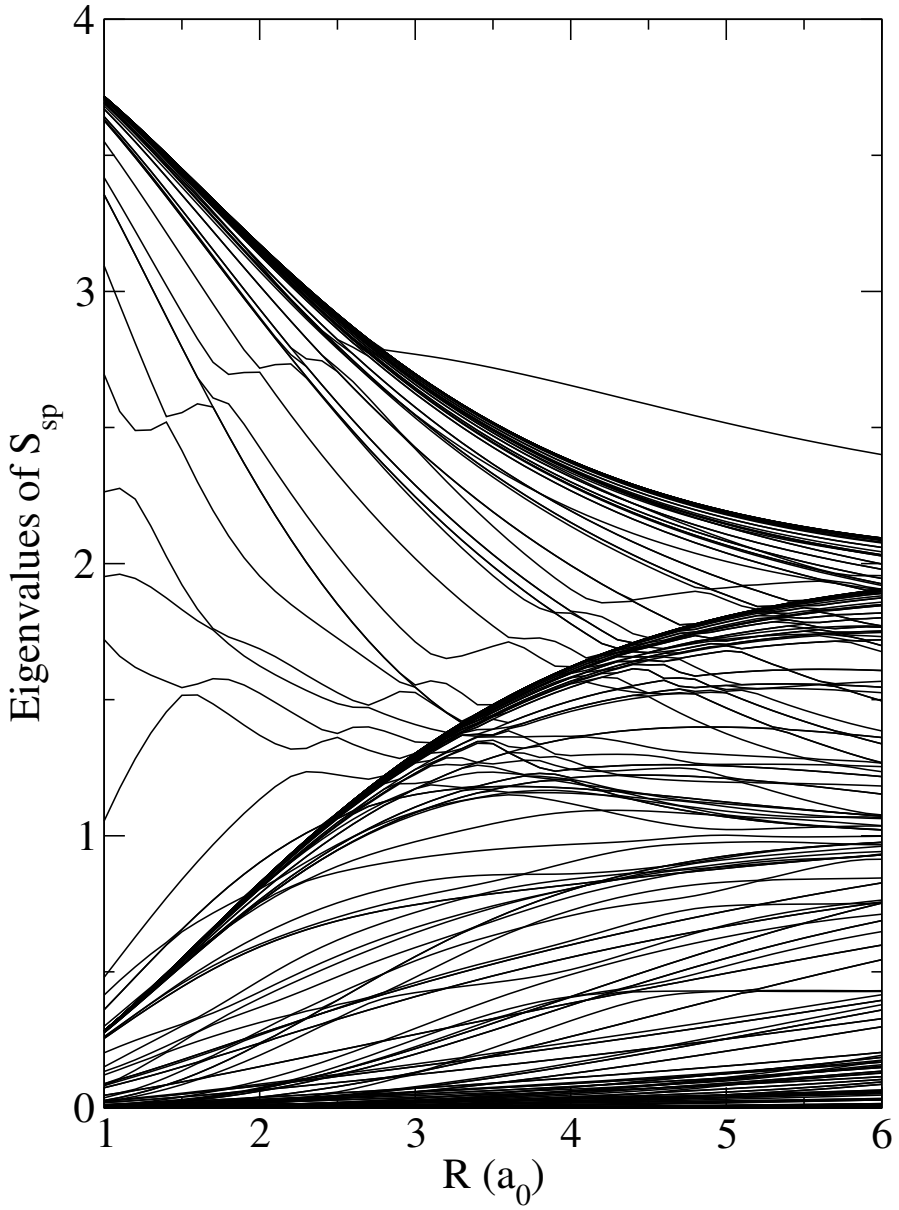

Figure 3. Eigenvalues of the singlet- and triplet-state metric matrix of Eq. (13) for diatomic hydrogen constructed in a $7s5p3d2f1g$ Sturmian Slater basis set,[27] including both covalent (119) and ionic or charge-transfer (154) terms. The origins of the structures evident in the plot, and of the spectral interval (0,4) in this case, are discussed in the text.

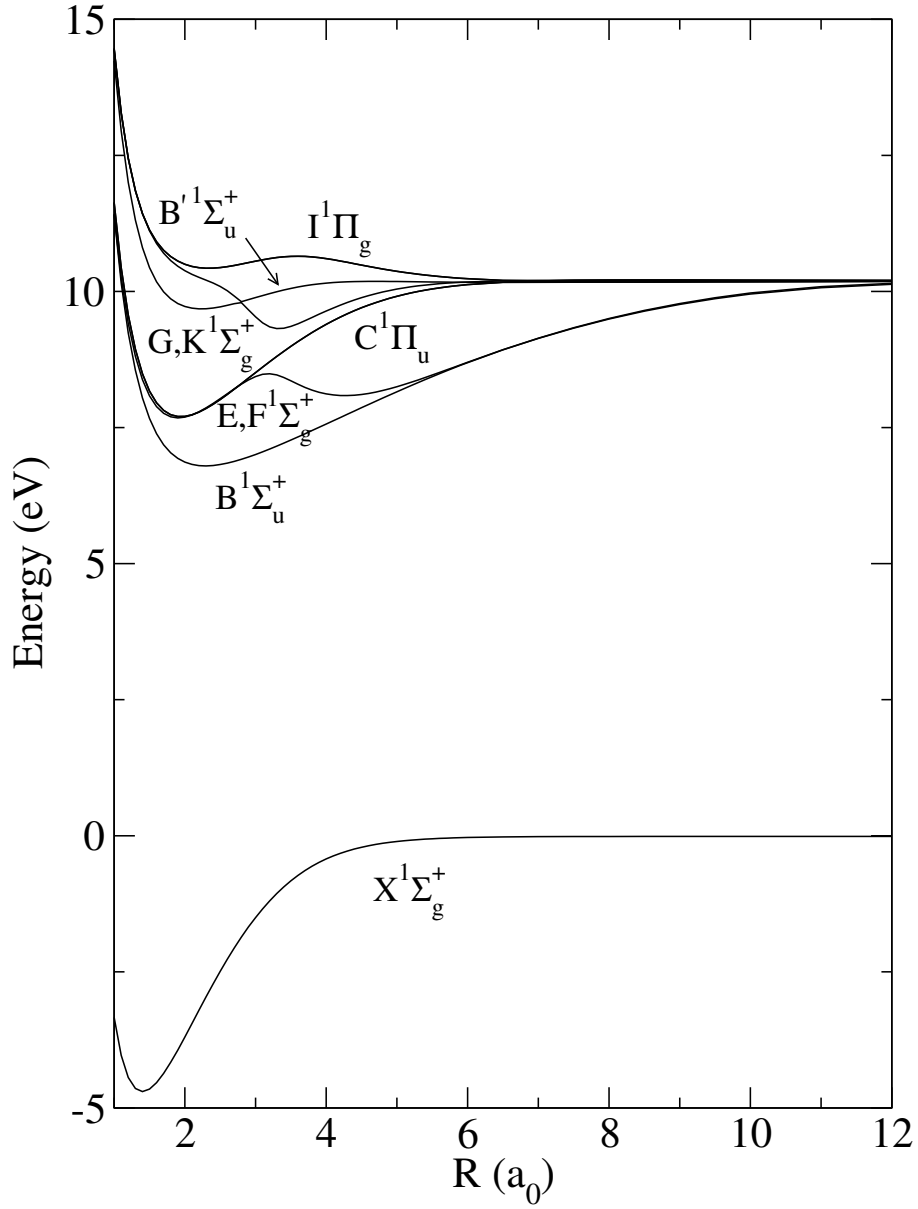

Figure 4. Singlet-state potential energy curves dissociating to n=1 and 2 limits in diatomic hydrogen, obtained from full (1953 terms) configuration-interaction calculations in an optimized $5s3p2d1f$ valence basis of Slater orbitals.[27]

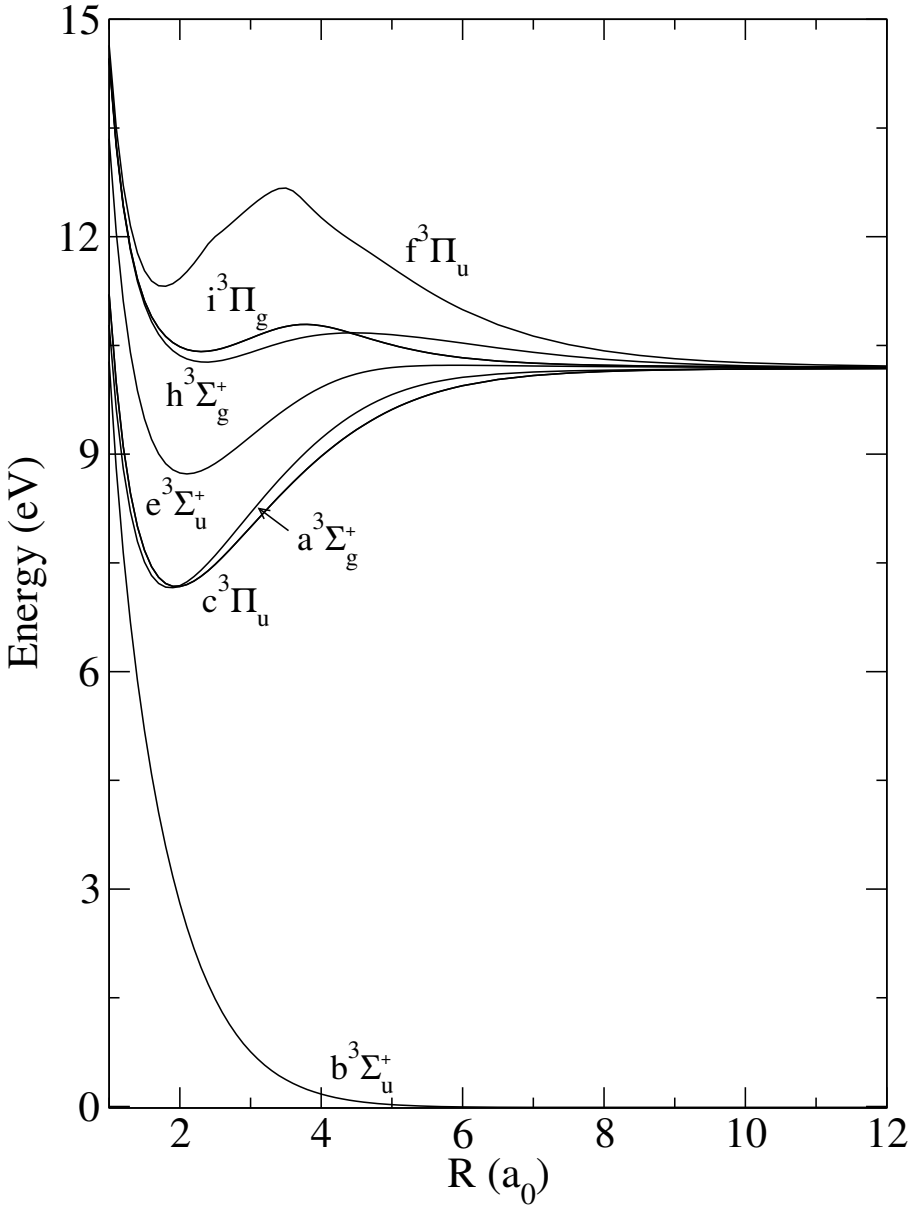

Figure 5. Triplet-state potential energy curves dissociating to n=1 and 2 limits in diatomic hydrogen, obtained from full (1891 terms) configuration-interaction calculations in an optimized $5s3p2d1f$ valence basis of Slater orbitals.[27]

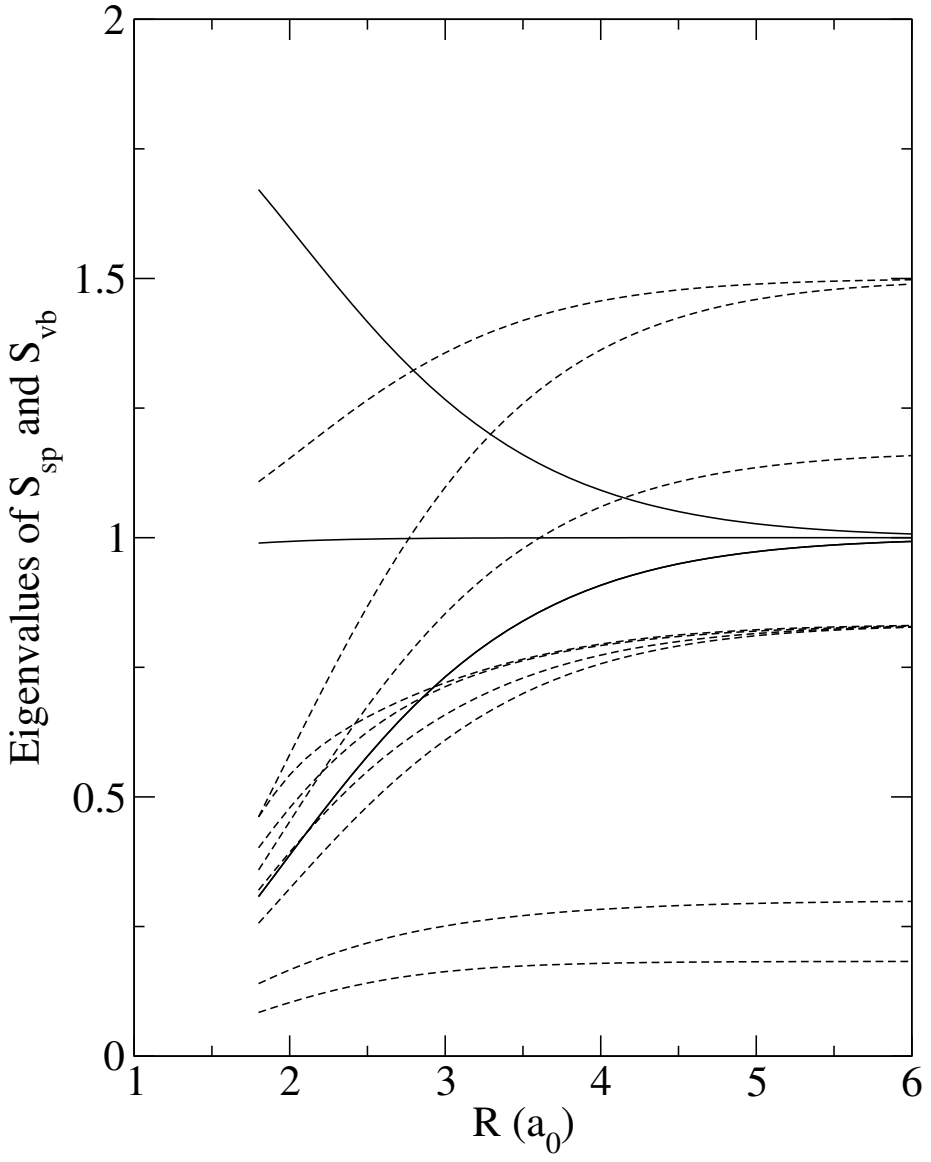

Figure 6. Eigenvalues of the doublet- and quartet-state metric matrix of Eq. (13) for diatomic CH, constructed employing hydrogen ($1s$) and carbon $1s^2(2s^22p^2 + 2s2p^3 + 2p^4)$ multiplet atomic configurations in an optimized valence orbital basis.[27] The solid lines refer to eigenvalues of the matrix in the orthonormal spectral-product representation, whereas the dashed lines are those obtained in the same configurational basis employing the normalization conventions of the standard tableau functions of valence-bond theory.[23]

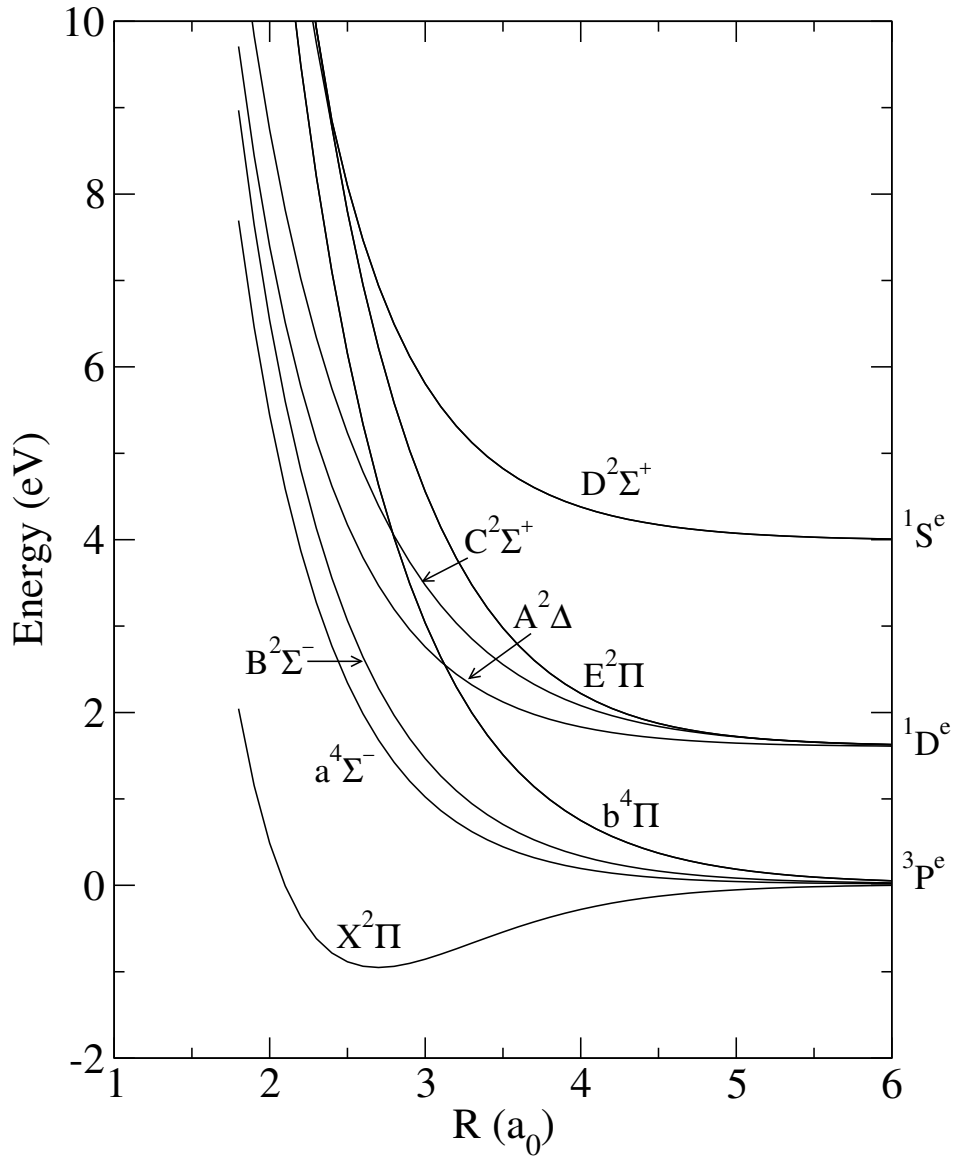

Figure 7. Potential energy curves for diatomic CH constructed employing minimal valence-shell multiplet carbon ($1s^2 2s^2 2p^2$) and hydrogen ($1s$) atomic configurations. The spectroscopic state labels employed follow conventions from experimental and previously reported theoretical studies.[13]

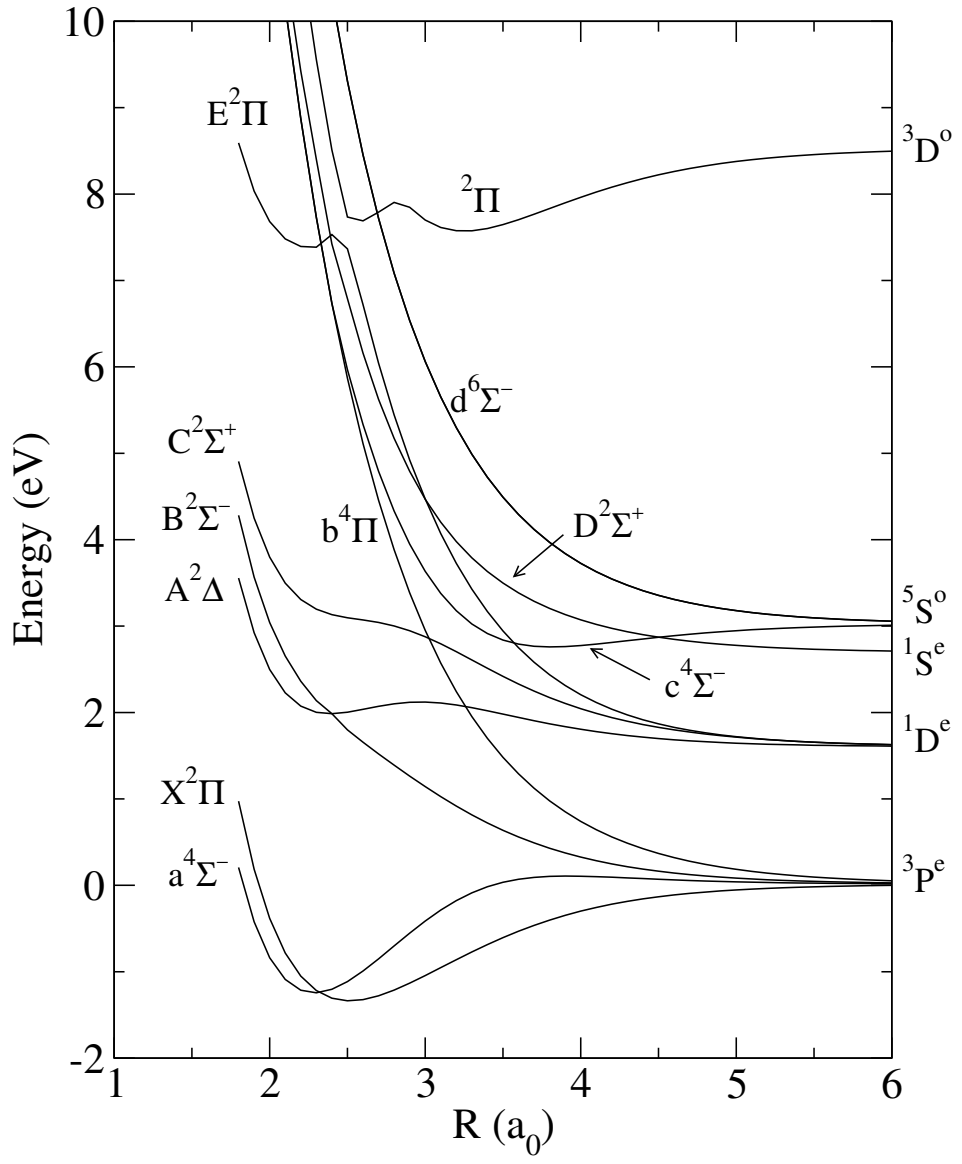

Figure 8. Potential energy curves for diatomic CH obtained in valence-shell multiplet carbon $1s^2(2s^22p^2 + 2s2p^3 + 2p^4)$ and hydrogen $(1s)$ atomic configurations. The state designations of the lower-lying curves are as in Figure 7, whereas the additional curves dissociating to the $^5S^o$ and $^3D^o$ carbon-atom limits are labeled employing conventional spectroscopic notation.[13]

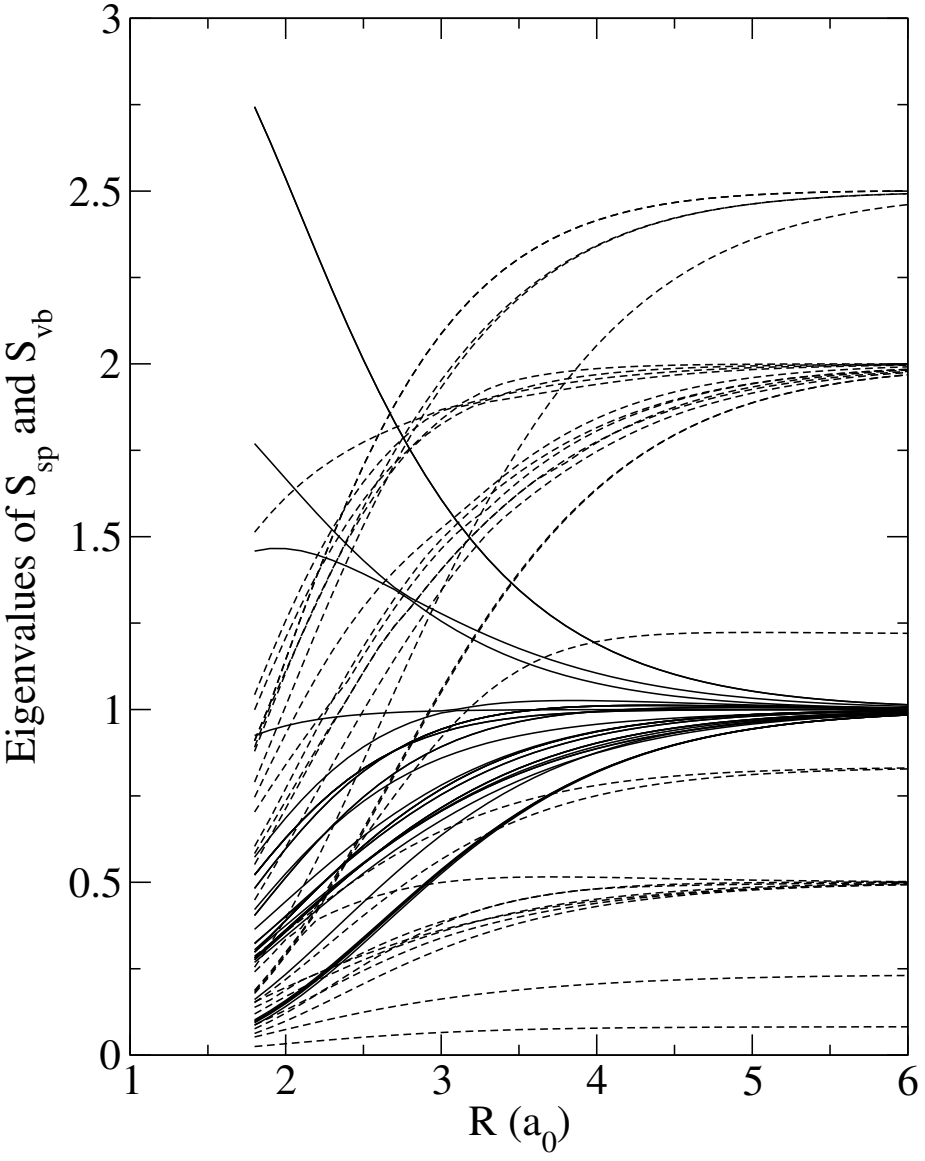

Figure 9. Eigenvalues of the singlet- and triplet-state metric matrix of Eq. (13) for symmetric collinear (H-C-H) methylene arrangements, constructed employing valence-shell multiplet carbon $1s^2(2s^2p^2 + 2s2p^3 + 2p^4)$ and hydrogen $(1s)$ atomic configurations. The solid lines refer to eigenvalues of the matrix constructed in the orthonormal spectral-product representation, whereas the dashed lines are those obtained in the same configurational basis employing the normalization conventions of the standard tableau functions of valence-bond theory.[23]

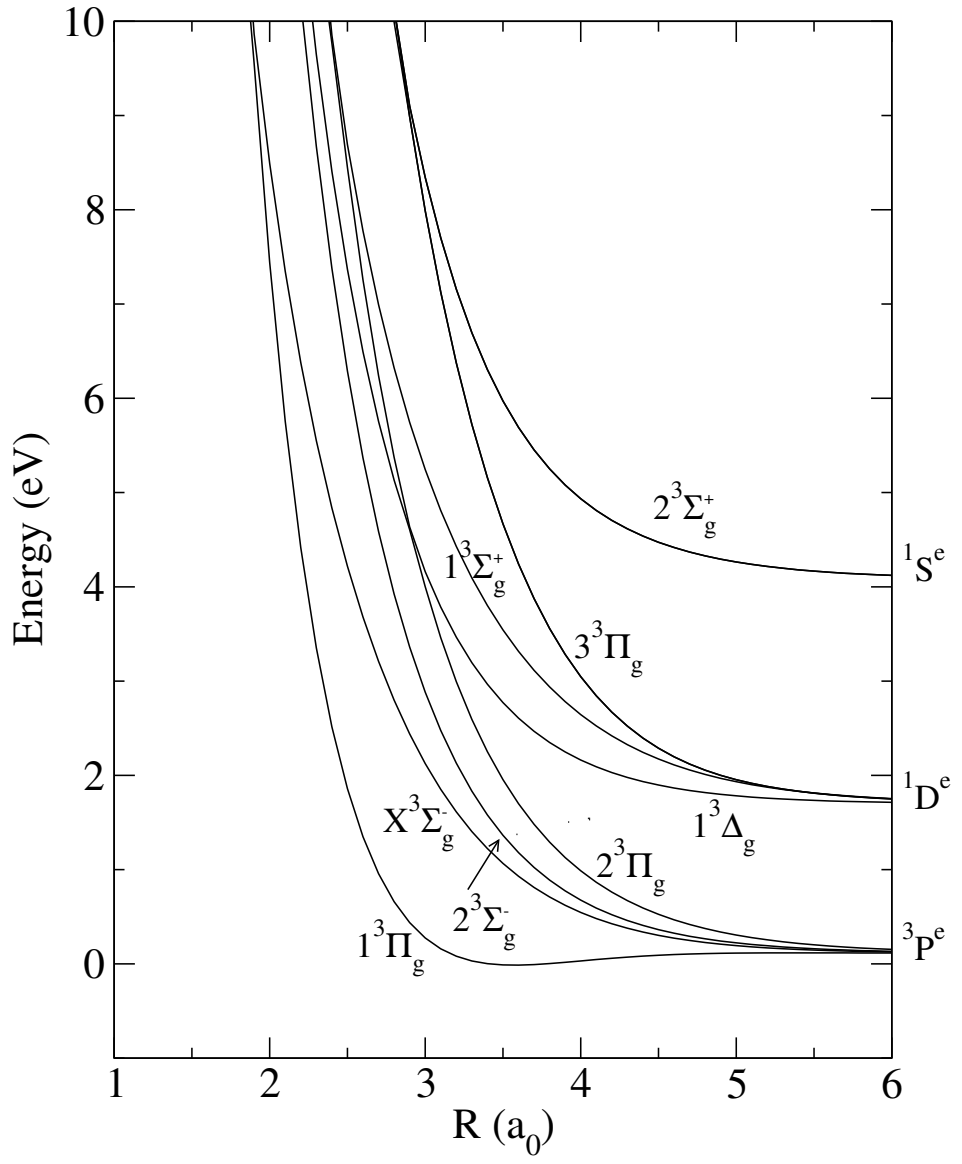

Figure 10. Potential energy curves for triplet methylene states in symmetric collinear (H-C-H) arrangements obtained in minimal valence-shell multiplet carbon ($1s^2 2s^2 2p^2$) and hydrogen ($1s$) atomic configurations. The ground $X^3\Sigma_g^-$ state is labeled on basis of experimental and previously reported theoretical studies,[14] whereas the other states are given sequential numerical labels.

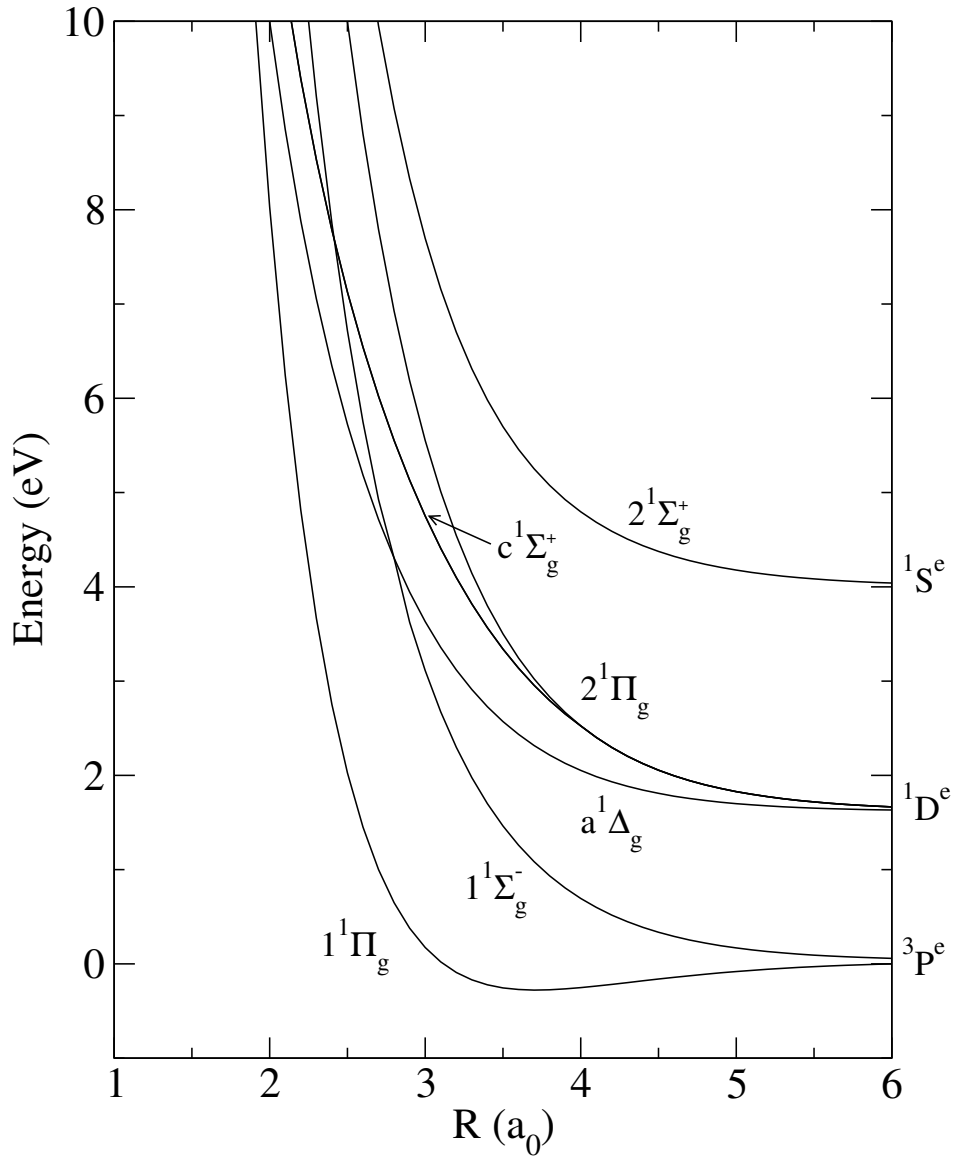

Figure 11. Potential energy curves for singlet methylene states in symmetric collinear (H-C-H) arrangement obtained in minimal valence-shell multiplet carbon ($1s^2 2s^2 2p^2$) and hydrogen ($1s$) atomic configurations. The two states given spectroscopic state labels follow conventions from experimental and previously reported theoretical studies,[14] whereas the other states are given sequential numerical labels.

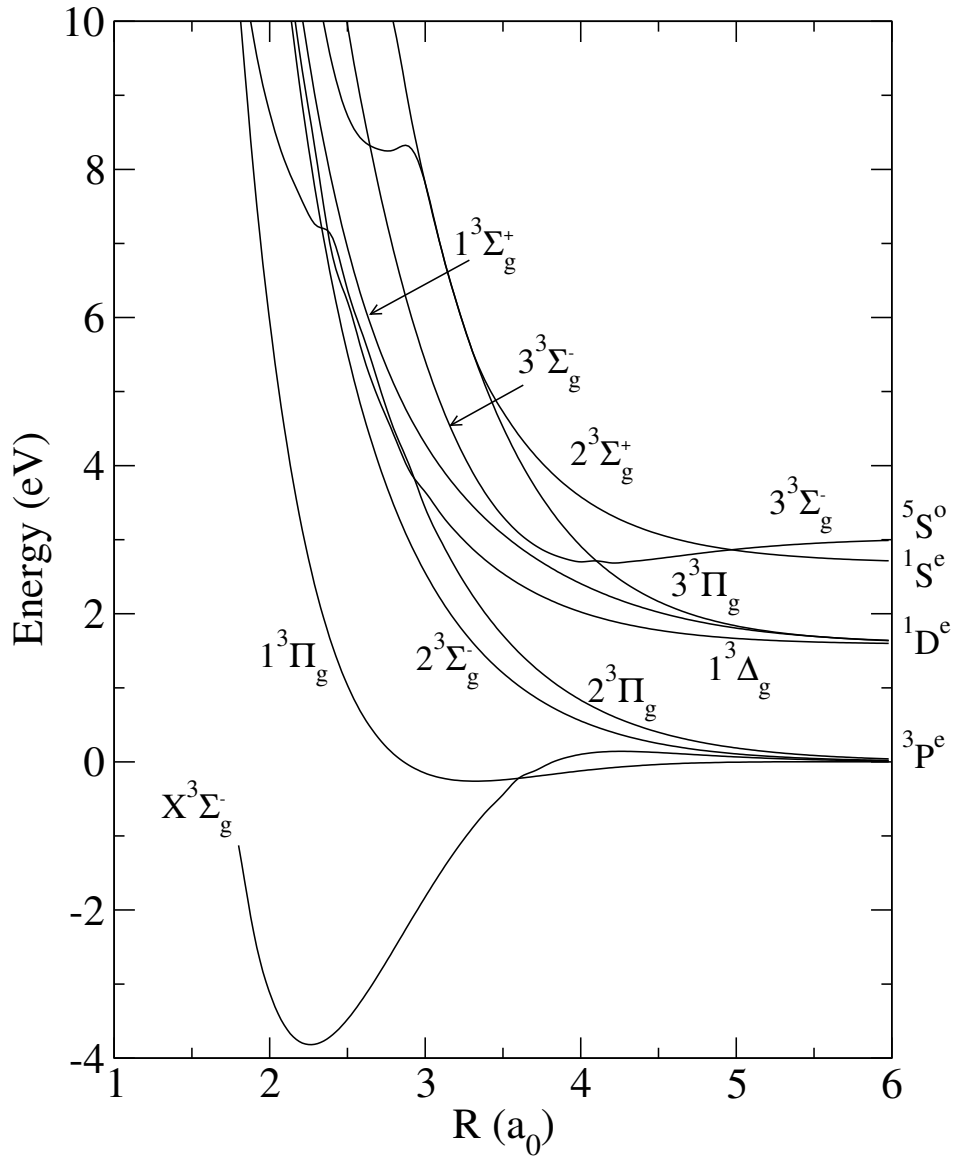

Figure 12. Potential energy curves for triplet methylene states in symmetric collinear (H-C-H) arrangements obtained in valence-shell multiplet carbon $1s^2(2s^22p^2+2s2p^3+2p^4)$ and hydrogen ($1s$) atomic configurations. The state designations of the curves are as in Figure 10.

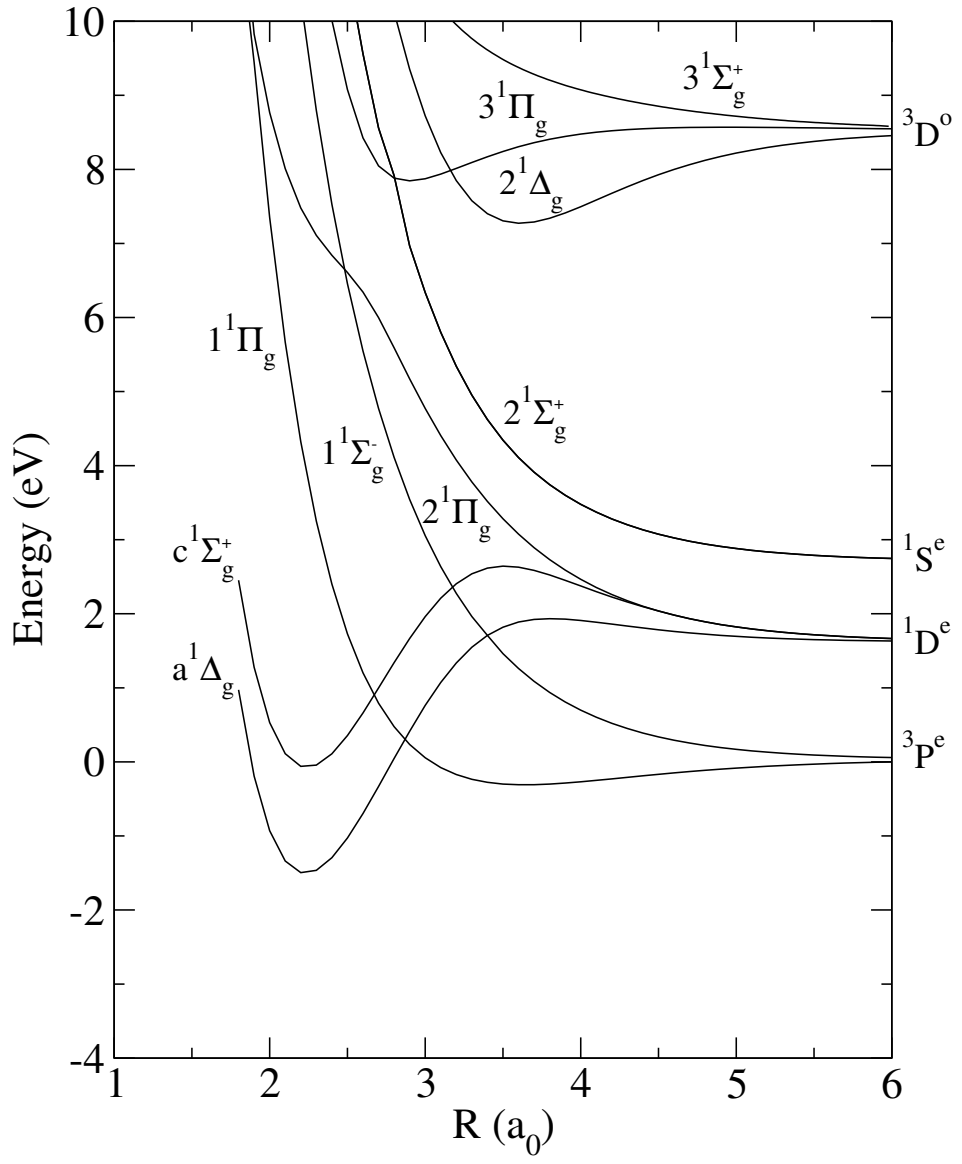

Figure 13. Potential energy curves for singlet methylene states in symmetric collinear (H-C-H) arrangement obtained in valence-shell multiplet carbon $1s^2(2s^22p^2 + 2s2p^3 + 2p^4)$ and hydrogen ($1s$) atomic states. The state designations of the curves are as in Figure 11.